



Customer: ESA/ESRIN
IDEAS +
Contract No
2016

Document Reference:

Issue Date: 15 December

Issue: 1.0

Project: Proba-V Clouds Detection Round Robin

Title: Proba-V Cloud Detection Algorithm Theoretical Basis Document

Author: Ute Gangkofner

Approval:

Table of Contents

1	Introduction.....	5
1.1	Background.....	5
1.2	Objective.....	5
2	Data	6
2.1	Proba-V Data	6
2.2	Auxiliary Data	8
3	Overview of Major Cloud Screening Methods	8
4	Proba-V Cloud Detection Algorithm developed.....	9
4.1	Model 1 - Retrieval of Clouds, Haze, Ice, and Snow.....	10
4.1.1	Cloud Model 1 - Part 1 – Derivation of Image Parameters	10
4.1.2	Cloud Model 1 - Part 2 – Derivation of Clouds, Haze, Snow, and Ice (undifferentiated).	15
4.2	Model 2 – Derivation of Image and Ancillary Parameters	17
4.3	Model 3 – Filtering and Reclassification.....	22
4.3.1	Filtering of the Safest Cloud Classes.....	23
4.3.2	Filtering of Classes 1 - 49	23
4.3.3	Filtering based on NDI of spectral band means and on Euclidean texture	25
4.3.4	Removing false clouds using large scale filters and ancillary information	27
4.3.5	Filling buffer pixels and gaps and adding clouds over water	27
4.3.6	Final cloud filtering.....	30
4.3.7	Separation of clouds and haze	31
4.4	Separation of ice and snow from clouds and haze.....	33
4.4.1	Derivation of an initial snow and ice mask.....	33
4.4.2	Reclassifying snow/ice at a large scale.....	34
4.4.3	Separating snow/ice patches from ice clouds.....	35
4.5	Correcting for the temporal shift of the SWIR band	37
5	Summary and Discussion.....	38
6	References.....	40

List of Figures

Figure 1: PROBA-V instrument layout. Source: [3].....	6
Figure 2: Spectral Response Function of per camera (Left, Center, Right). Source: http://proba-v.vgt.vito.be/content/spectral-response-functions	7
Figure 3: Proba-V imagery, 4 examples out of 330 used for the cloud mapping.....	7
Figure 4: Flowchart of the presented algorithm	9
Figure 5 Overview of the first cloud processing model (ERDAS Spatial Model Editor).....	10
Figure 6: Examples of the differences within a single image, using the band combination SWIR-NIR-Blue (RGB).....	11
Figure 7: Examples of some of the generated image parameters, as references the Proba-V red band is shown in the upper left image. The image is part of probav_l2a_20140621_074105_2_333m_v001.tif shown in Figure 6	12
Figure 8: Cloud Model 1, Part 1c: derivation of texture based parameters	13
Figure 9: Example of cloud and haze enhancement with Euclidean texture parameters	13
Figure 10: Example of the cloud classification result of Cloud Model 1 with 66 undifferentiated classes (that is every class may include clouds, haze, ice, or snow). The commission errors increase with the higher classes (towards yellow and reddish tones) with decreasing brightness of the features. The right hand colour bar in the middle of the left hand column refers to the class aggregation (parameter 9 in Table 2), the lowest colour legend belongs to the final result.....	17
Figure 11: Model for derivation of the image and ancillary parameters used for Model 2 (filtering) .	17
Figure 12: Reclassified CCI LC (2010) with large lakes in light blue and smaller water bodies in yellow	21
Figure 13: Overview of the second cloud processing model (ERDAS Spatial Model Editor).....	22
Figure 14: Central part of image probav_l2a_20140621_174841_2_333m_v001.img (SWIR-NIR-Blue RGB) with image parameter euctext_cv_mult100.img (no. 8 in Table 2) in the lower image. Haze and small clouds have very low values and can be readily enhanced with this image parameter	25
Figure 15: Comparison of first classification result of clouds over water to final result after adding water based on the mean euclidean distance texture parameter.....	30
Figure 16: Differentiation of clouds (magenta) and haze (yellow) (probav_l2a_20140321_044105_3_333m_v001.img).....	32
Figure 17: Example of snow/ice (blue) and thin/partial snow/ice (cyan) classes in image probav_l2a_20140321_094455_3_333m_v001.tif of the Alps (March 21, 2014). Magenta: clouds, light pink: haze	36
Figure 18: Effect of the correction of the SWIR shift	38

List of Tables

Table 1: Input parameters derived for cloud detection in Model 1.....	14
Table 2: Input parameters derived in Model 2 for usage in Model 3	18
Table 3: Filtering classes 1-15.....	23

Table 4: Filtering classes 1-49..... 24

Table 5: Filtering based on NDI of spectral band means and on Euclidean texture 26

Table 6: Removing false clouds based on large scale parameters and ancillary information 27

Table 7: Filling buffer pixels and gaps and retrieving more clouds over water 28

Table 8: Removal of Unlikely Clouds 30

Table 9: Separation of clouds and haze..... 31

Table 10: First step of snow and ice retrieval 33

Table 11: Reclassifying snow and ice in large area buffers 34

Table 12: Correction of the SWIR shift 37

Change Records

Date	Version	Change Record	Author
16.02.2017	1.0	ATBD Version 1.0	Ute Gangkofner

Acronyms and Abbreviations

AD	Applicable Documents
CCI	Climate Change Initiative
EO	Earth Observation
LAI	Leaf Area Index
LC CCI	Land Cover Climate Change Initiative
NDVI	Normalized Difference Vegetation Index
NDI	Normalized difference Index
NIR	Near Infrared
SWIR	Short Wave Infrared
TIR	Thermal Infrared
TOA	Top-of-atmosphere

Applicable Documents and Web Links

- [AD 1] Jannone, R. (2016), Proba-V Clouds Detection Round Robin Protocol v 2.0
- [AD 2] Stelzer, K., Paperin, M. Kirches, G. (2016), Proba-V Clouds Round Robin, Description of the Test Data Set v 1.2
- [AD 3] <https://earth.esa.int/web/sppa/activities/instrument-characterization-studies/pv-cdrp/project-documents>

1 Introduction

1.1 Background

This ATBD describes a cloud detection approach developed under a Round Robin exercise on Proba-V cloud detection (PV-CDRR) that was organized by the European Space Agency (ESA) in collaboration with the Belgian Science Policy Office (BELSPO).

As laid out in the Proba-V Clouds Detection Round Robin Protocol [AD 1] cloud detection for Proba-V is currently based on multiple thresholds method applied to the Blue and the SWIR spectral bands [1]. [AD 1] states: *“The drawback of such thresholds method is that its accuracy depends on the amount of contrast in radiometry between the underlying surface and the clouds. Owing to the heterogeneity of the surface reflectance characteristics, the definition of a globally valid threshold is practically impossible. To overcome this limitation, a new algorithm was recently developed and it is now being implemented for next Proba-V reprocessing [RD 3]. The new algorithm uses monthly means of reflectance in the blue band and associated status maps derived from MERIS FR mission. This auxiliary information is used to design a “dynamic threshold” algorithm, with cloud tests customized for each status class (land, water, snow/ice, unknown land cover)”*. The new algorithm is described in [2].

In order to address still remaining issues (in particular a dependence on illumination and viewing geometry and some remaining misdetection at the edges of each status class (e.g., land/water)) and define the baseline for the future operational processor, the Round Robin exercise was initiated.

To support the common understanding of the different cloud, snow/ice and haze species and their appearance in the images and to give orientation about the validation dataset, a test data set was provided to the Round Robin Participants along with a documentation [AD 2]. The test data set consists of 1350 labelled pixels with detailed information on cloud types, etc. The final validation data set is planned to contain over 40.000 pixels and will be the validation basis for all algorithms.

1.2 Objective

The reliable retrieval of clouds, ice/snow and haze is critical for most applications of EO data. The quality of automatic mosaicking of EO data or temporal compositing and the correctness of quality labels for instance rely fundamentally on the correct extraction of clouds in combination with the description of atmospheric conditions. While several sensors carry specific cloud and atmosphere sensitive bands on board (TIR channels or dedicated cirrus band as the 1.38 micron band), cloud screening with Proba-V is confined to its four spectral bands (Blue, Red, NIR and SWIR, see [4]) and the nonetheless existing cloud/ice/haze sensitivity of these.

The objective of this particular cloud detection algorithm is to reach the highest possible cloud/ice/haze mapping accuracy based largely on the Proba-V data alone (some exceptions are described in 2.2), in order to obtain a benchmark for this approach. Of the possible three error types with regards to clouds, i.e., omission, commission and wrong labelling of clouds/haze (snow/ice instead of clouds or vice versa), the avoidance of omission errors was considered the first priority. Omission errors may lead to wrong image data signals because bad data are taken for good, while commission errors (clouds/haze mapped, but none existent) and wrong labelling are thought to have less severe consequences: wrong labelling will at least enable a proper disregarding of data for certain applications (where neither ice/snow nor clouds/haze should be contained), while commission errors may invoke data replacement by other suitable scenes, even though it would have not been necessary.

In the future, the algorithm may be further improved with the main objective to mitigate certain commission and class confusion errors either by further algorithm improvements based on the Proba-V data or/and the usage of additional information.

2 Data

2.1 Proba-V Data

The input test scenes that have been processed (and that have been provided to all participants) are Proba-V TOA products. More specifically, Level 2a products are used, consisting of TOA reflectances in the four Proba-V bands, radiometrically and geometrically corrected, in geographic coordinates, and provided as full segments (not tiled) and resampled to the chosen spatial resolution of 333m. The data cover the entire globe on four days representing the four seasons and consist daylight measurements of land and coastal areas. Figure 4 shows an example of four Proba-V images overlaid on the aggregated CCI LC map.

“Level 2a products are scenes generated by Level 1c data and therefore they are provided by individual cameras. Depending on the camera, the swath covered by the Level 2a products changes; the area covered by the central camera is about 500 km, whereas the area covered by the left and right cameras is of the order of 875 km. They slightly overlap in the across-track direction” [AD 1].

The following dates are covered with a total of some 330 single data sets provided in HDF5 format:

- 21/03/2014
- 21/06/2014
- 21/09/2014
- 21/12/2014

Figure 2 shows the Proba-V instrument layout, Figure 2 the spectral response functions of the four spectral bands per left, center and right camera.

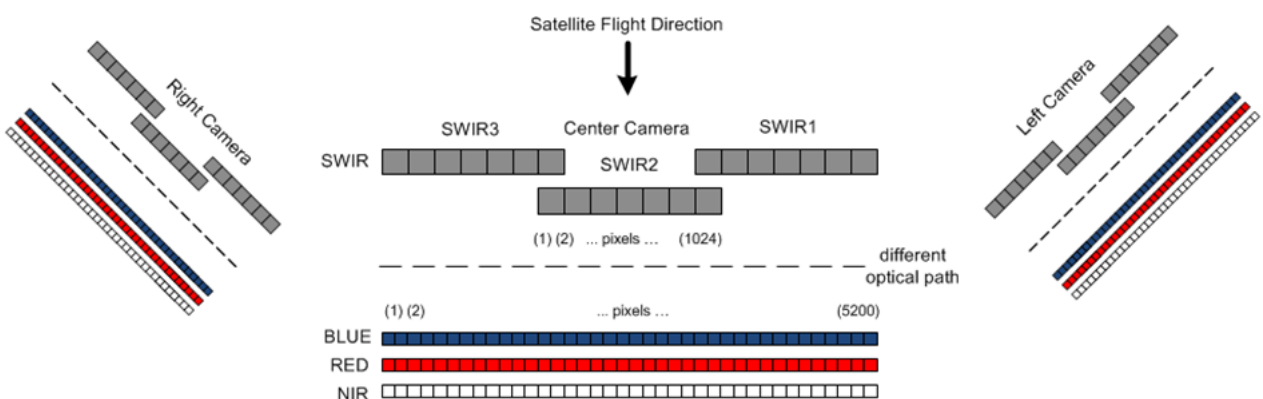


Figure 1: Figure 2: PROBA-V instrument layout. Source: [3]

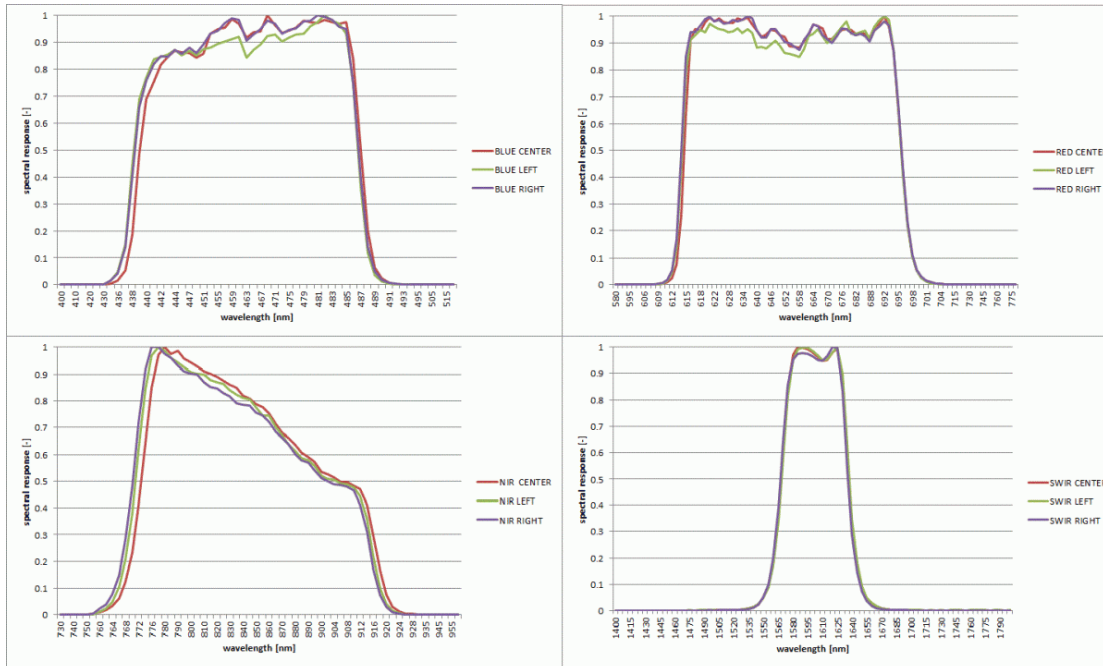


Figure 3:

Spectral Response Function of per camera (Left, Center, Right). Source: <http://proba-v.vgt.vito.be/content/spectral-response-functions>

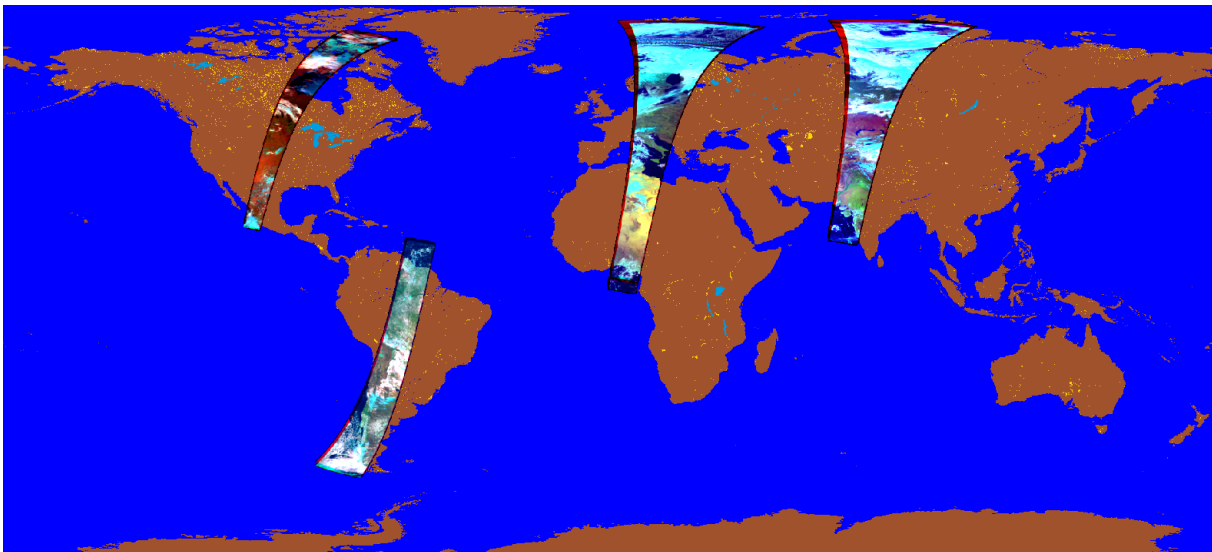


Figure 4: Proba-V imagery, 4 examples out of 330 used for the cloud mapping

While the viewing angles of the three cameras vary wildly, the spectral response functions between the cameras look rather consistent. In the cloud detection algorithm developed here, the viewing and illumination geometry has not explicitly been considered, i.e. by directly modelling their expected effects.

A definite issue for the cloud detection is the temporal shift between the recordings of the different spectral bands: “... the NIR observes a cloud first, followed by the RED, BLUE, and SWIR bands. The time difference between the NIR and SWIR cloud observation is 12 s. As a result, the NIR and SWIR bands will map clouds onto different positions in the along-track direction, with differences up to ~700 m for clouds at 10 km altitude. Other effects of the different observation times include viewing angle

differences and horizontal cloud shifts. The maximum shift resulting from the latter two effects will not exceed three 1/3 km pixels along-track and one pixel cross-track on either side “ [3, p. 17].

In practice this means that the clouds are defined by the common cloud area of the four spectral bands, plus the cloud area affected by the temporal shift. In [3] the authors describe how they cope with this fact via a threshold / moving window based approach.

2.2 Auxiliary Data

The here presented algorithm is largely based on the Proba-V data only. Nevertheless, in addition CCI LC (Land Cover data of the ESA Climate Change Initiative [4]) were used for various purposes, as will be described below (see 4.2). These data originate from ENVISAT MERIS data and cover the full globe at 300m resolution, matching well the Proba-V resolution used. Only water bodies and their derived boundaries were included in the algorithm (see Table 2).

3 Overview of Major Cloud Screening Methods

Cloud detection methods applicable to remote sensing data vary broadly and depend besides the EO data used on the purposes and priorities related to the usage of the EO data. Also, combinations of different methods are found, and may in the end bear the best chances for accurate cloud and snow/ice mapping. Some examples are presented here to highlight some basic retrieval mechanism.

The dominant approaches in practice may still be threshold based approaches, where various combinations of spectral bands and derivatives such as band ratios or normalised difference indices or other band combinations are used to describe the multispectral behaviour of clouds. The above mentioned approaches for Spot Vegetation and then Proba-V are such approaches [1], [2], where the modified threshold method of [2] is more sophisticated: based on monthly means of reflectance in the blue band and associated status maps derived from MERIS data a “dynamic threshold” algorithm has been developed, with cloud tests customized for each status class (land, water, snow/ice, unknown land cover) [AD 1].

Another principle of cloud detection is based on analysis of multitemporal anomalies. Such work was recently presented by [3] in the context of time series based Proba-V LC mapping, where the authors used temporal filtering algorithms. Especially dense time series data enable such approaches, but references are also made to Landsat based multitemporal approaches [6].

[7] describe a Bayesian Cloud Detection Scheme developed for Along-Track Scanning Radiometer (ATSR) data. Referring to the drawbacks and general weaknesses of threshold based approaches, the authors calculate a probability of clear-sky to each pixel, which allows the end user to select their own tolerance for cloud contamination depending on their particular application. The Bayesian calculation assigns this probability based on satellite observations and prior Numerical Weather Prediction (NWP) information.

A whole arsenal of tests and auxiliary data is applied to the MODIS cloud detection. It leads to a clear-sky confidence level (high confident clear, probably clear, undecided, cloudy). The spectral tests within the methodology rely on radiance (temperature) thresholds in the infrared and reflectance thresholds in the visible and NIR. Thresholds vary with surface type, atmospheric conditions (moisture, aerosol, etc.), and viewing geometry [8].

4 Proba-V Cloud Detection Algorithm developed

The presented cloud detection algorithm consists of three major steps, which have been implemented in three models, developed with the Spatial Model Editor of ERDAS IMAGINE 2016.

1. In the first model, the clouds, haze, ice/snow pixels are captured aiming at a complete retrieval.
2. The second model derives all image and ancillary parameters that are used for the filtering of the clouds, haze, ice/snow pixels and their class separation.
3. In the third model the still undifferentiated clouds, haze, and ice/snow pixels are filtered in order to eliminate commission errors. In addition, the third model separates clouds from haze, as well as ice/snow from clouds and haze.

The three models are described in detail in the next sections. A flowchart of the overall algorithm is shown in Figure 5.

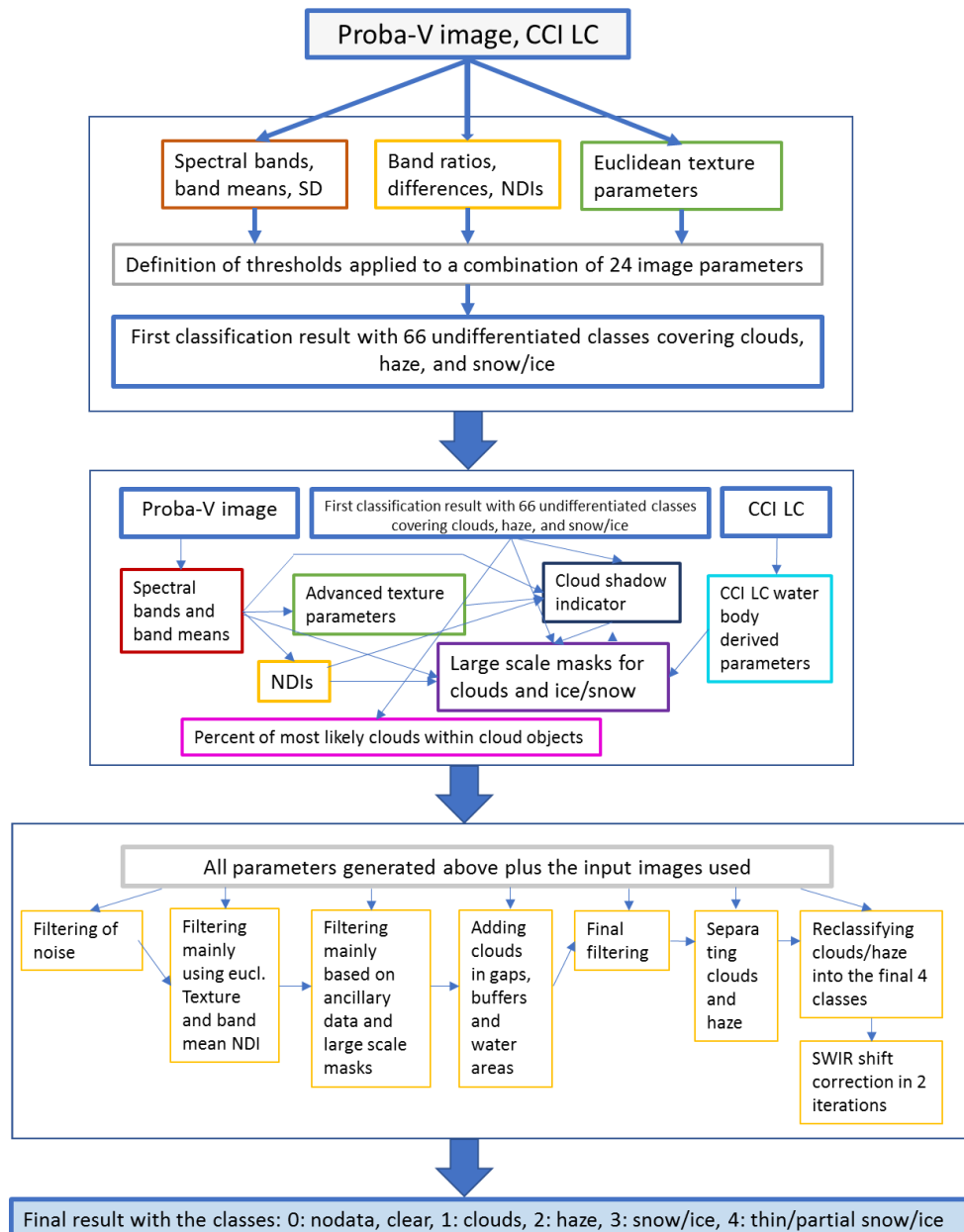


Figure 5: Flowchart of the presented algorithm

4.1 Model 1 - Retrieval of Clouds, Haze, Ice, and Snow

Figure 6 provides an overview of the first cloud processing model. Its main parts are comprised of:

1. Derivation of three sets of image parameters consisting of the four Proba-V input bands, ratios, normalized difference images, band differences, and texture parameters.
2. Deriving thresholds to all or parts of these parameters and thereby defining a total of 66 classes containing clouds, snow, ice, and haze. The derived classes are not yet differentiated into clouds, haze, etc. in model1.

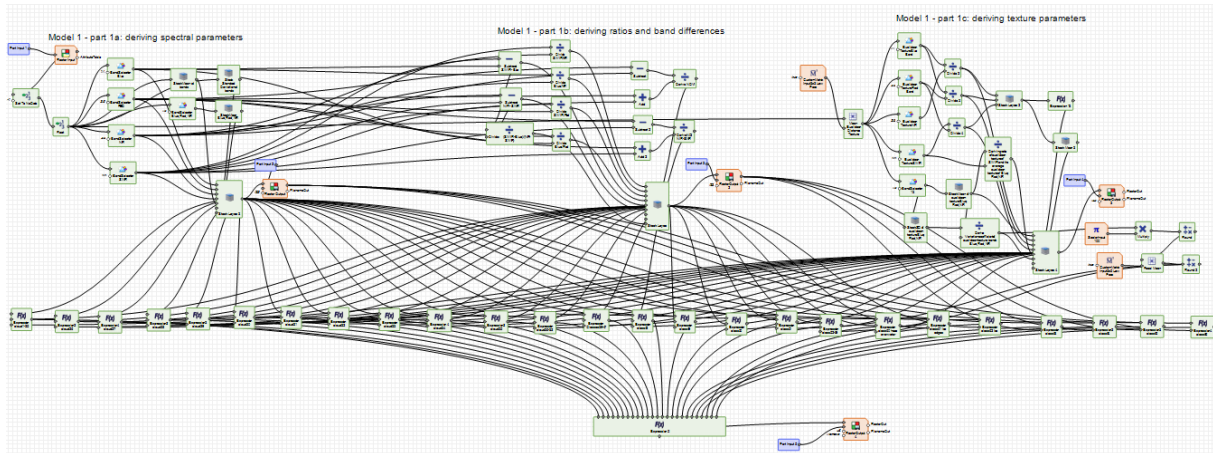


Figure 6 Overview of the first cloud processing model (ERDAS Spatial Model Editor)

The following sections describe the three parts of the first cloud processing model.

4.1.1 Cloud Model 1 - Part 1 – Derivation of Image Parameters

Three sets of Proba-V image based parameters were derived, as described below.

Table 1 provides a summary of the image parameters used. Not all of these parameters are used in all thresholding operations for the 66 initial classes, especially not for the definition of the first, brightest classes, which rely much more on the spectral parameters than on the derived ratios (or band differences and NDIs) or the texture parameters. However, with increasing class number and decreasing brightness of the classes, these additional parameters become more and more important, as the resulting classes cover increasingly mixed pixels consisting of the spectral properties of the ground and of clouds (or ice/snow).

4.1.1.1 Cloud Model 1 - Part 1a – Derivation of Spectral Parameters

The following spectral parameters were derived and used for the cloud extraction as well as (partly) for the subsequent filtering and clouds/ice separation:

- a) The four spectral Proba-V bands: blue, red, NIR, SWIR
- b) The average of blue, red, and NIR
- c) The average of blue, red, NIR, and SWIR
- d) The standard deviation of blue, red, NIR, and SWIR
- e) The average of blue, red, and NIR

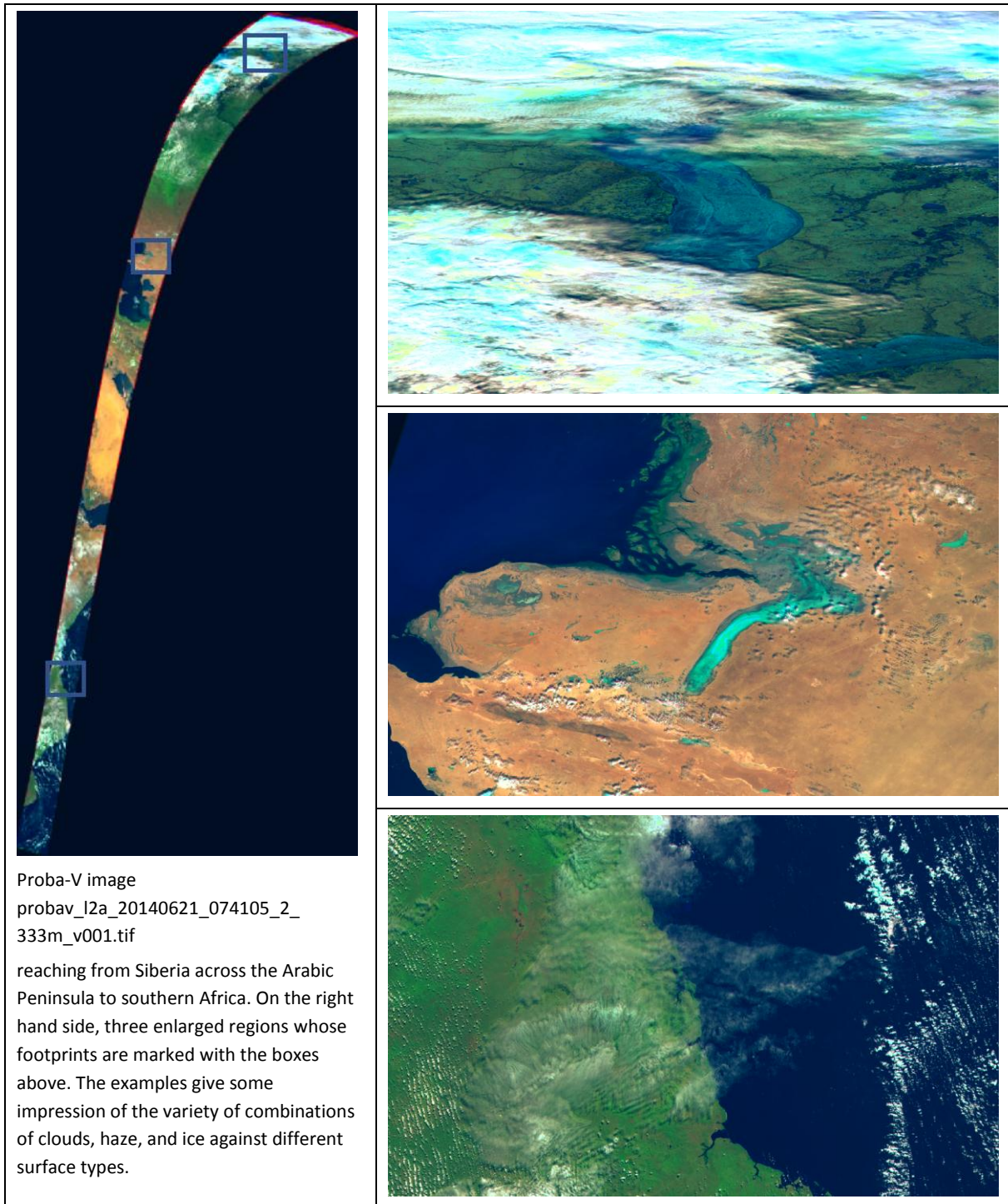


Figure 7: Examples of the differences within a single image, using the band combination SWIR-NIR-Blue (RGB)

The above Figure 7 provides an example of the heterogeneity of the clouds, haze and ice surfaces found within such image segments spanning the land surface from North to South of the entire globe.

4.1.1.2 Cloud Model 1 - Part 1b - Derivation of Ratios and Band Differences

The second set of Proba-V image derived parameters comprises band ratios including normalized difference ratios and band differences.

The following ratio and difference parameters were derived and used for the cloud extraction as well as (partly) for the subsequent filtering and clouds/ice separation:

- a) Band Ratio SWIR/NIR
- b) Band Ratio Blue/NIR
- c) Band Ratio SWIR/Red
- d) Band Ratio Blue/Red
- e) Band Difference SWIR – Blue
- f) Band Difference NIR – SWIR
- g) NDVI (Normalized Difference Vegetation Index)
- h) NDI (Normalized Difference Index) NIR-SWIR (also referred to as Normalized Difference Water Index – NDWI)
- i) Ratio of the two difference images: (SWIR-Blue) / (NIR-SWIR)

The selection of the ratios, band differences and NDIs and the applied thresholds were empirically determined, by thoroughly studying the multispectral properties of the images. In many cases classical training samples were defined in order to extract the statistical parameters of the defined classes. Figure 8 shows some examples of the multispectral indices along with the red band for reference.

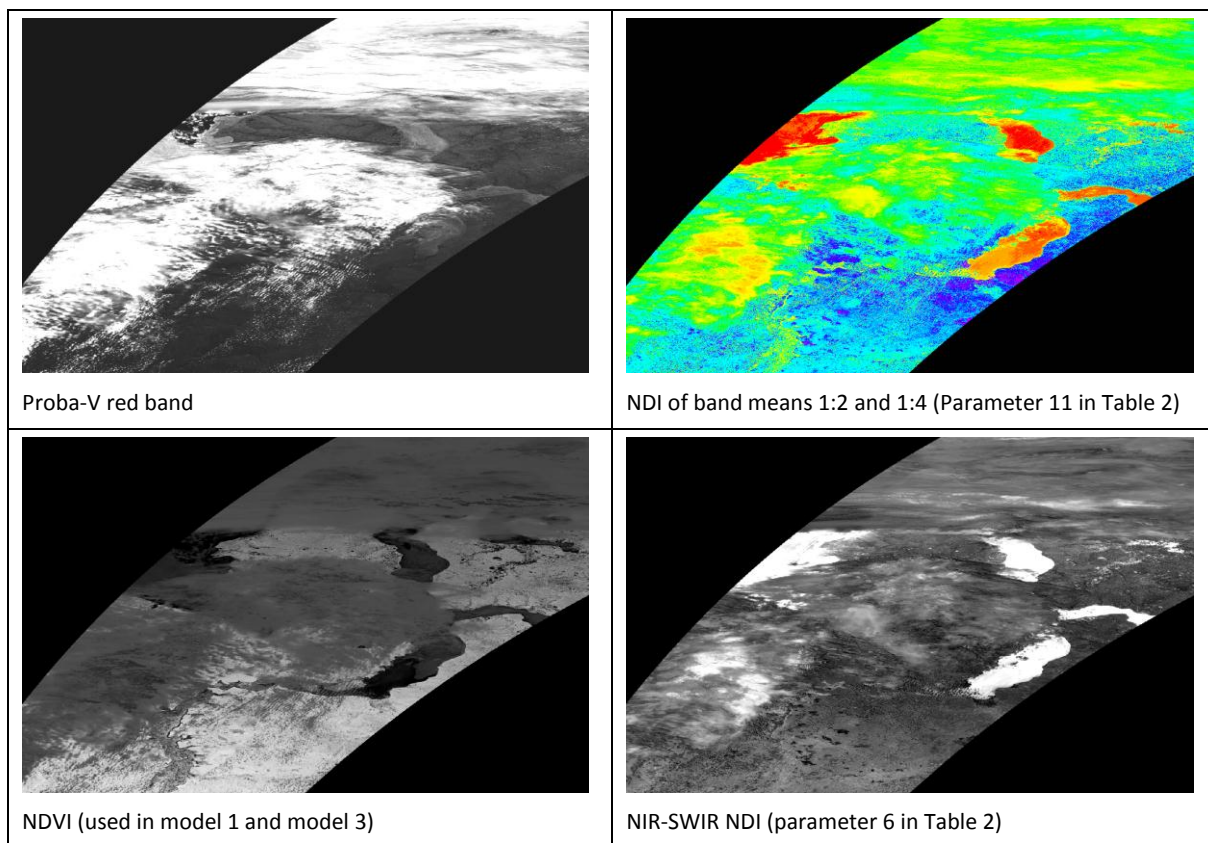


Figure 8: Examples of some of the generated image parameters, as references the Proba-V red band is shown in the upper left image. The image is part of probav_l2a_20140621_074105_2_333m_v001.tif shown in Figure 7

4.1.1.3 Cloud Model 1 - Part 1c - Derivation of texture based parameters

The third set of Proba-V image derived parameters is comprised of Euclidean texture based parameters. The mean Euclidean texture was calculated for each spectral band in 3x3 pixel windows, and several parameters were derived, as shown in Figure 9.

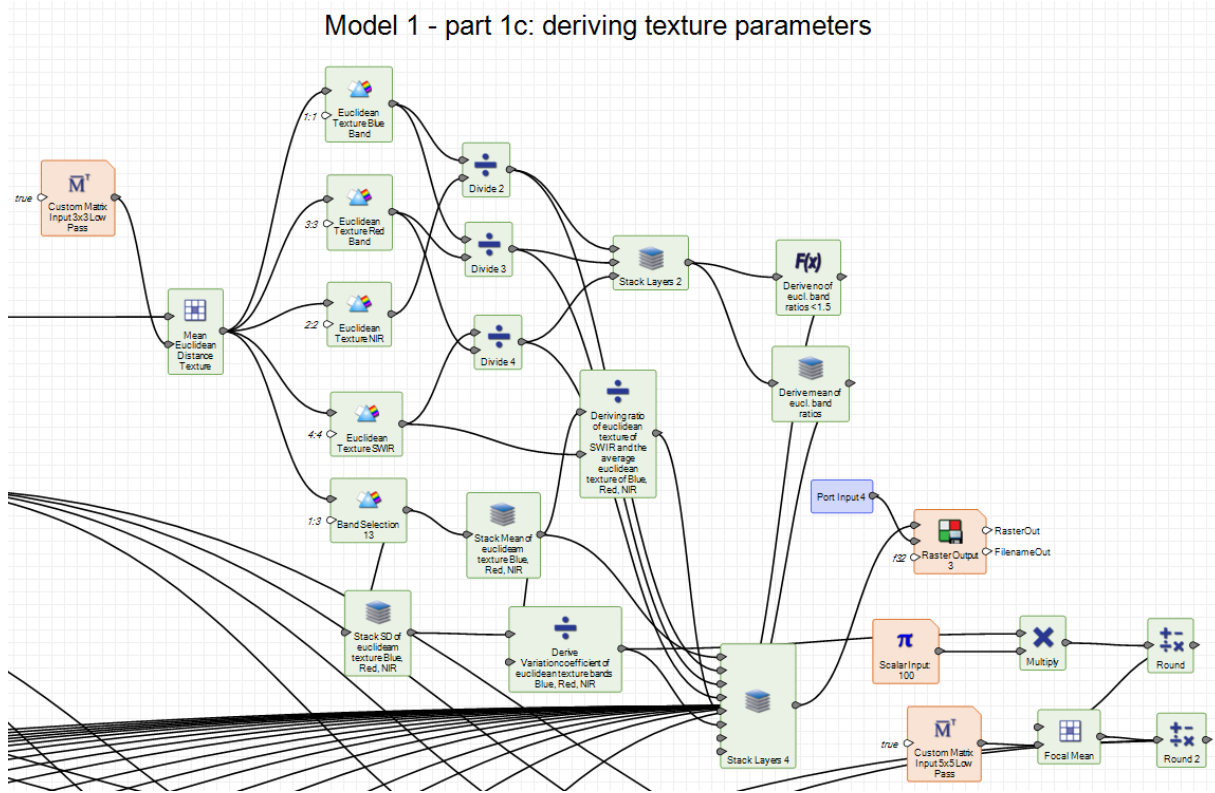
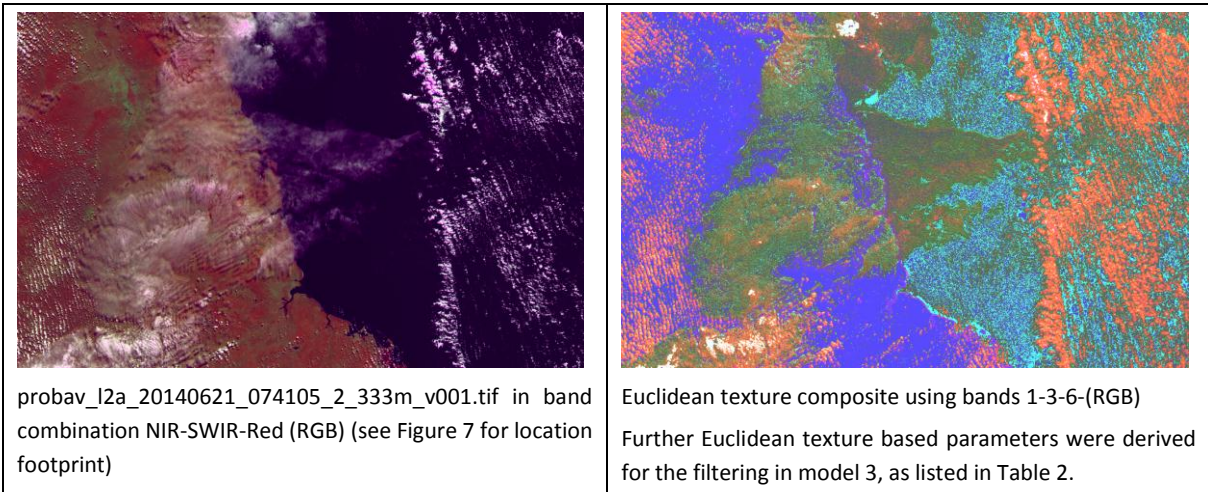


Figure 9: Cloud Model 1, Part 1c: derivation of texture based parameters

The following Euclidean texture based parameters were generated:

- a) Mean of the euclidean texture bands of the Blue, Red and NIR spectral bands
- b) Ratio of the euclidean texture of the Blue and the NIR bands
- c) Ratio of the euclidean texture of the Blue and the Red bands
- d) Ratio of the euclidean texture of the SWIR and the Red bands
- e) Ratio of the euclidean texture of the SWIR band and the mean of the euclidean texture bands of the Blue, Red and NIR spectral bands
- f) Variation coefficient of the euclidean texture bands of the Blue, Red and NIR spectral bands
- g) Number of euclidean band ratios that are smaller than 1.5
- h) Mean of euclidean band ratios



probav_l2a_20140621_074105_2_333m_v001.tif in band combination NIR-SWIR-Red (RGB) (see Figure 7 for location footprint)

Euclidean texture composite using bands 1-3-6-(RGB) Further Euclidean texture based parameters were derived for the filtering in model 3, as listed in Table 2.

Figure 10: Example of cloud and haze enhancement with Euclidean texture parameters

Figure 10 shows an example of the cloud and especially haze enhancement effect of the Euclidean texture derived image parameters. Another example is provided in Figure 14.

Table 1 provides a list of all image parameters used for the cloud detection in Model 1.

Table 1: Input parameters derived for cloud detection in Model 1

No	Parameters used for cloud detection	Description
1	Proba-V band 1	TOA reflectance in the blue band
2	Proba-V band 2	TOA reflectance in the red band
3	Proba-V band 3	TOA reflectance in the NIR band
4	Proba-V band 4	TOA reflectance in the SWIR band
5	$(Blue + Red + NIR + SWIR)/4$	Average of the 4 reflectance bands
6	Standard deviation of bands 1-4	Standard deviation of the 4 reflectance bands
7	$(Blue + Red + NIR)/3$	Average of the blue, red and NIR bands
8	$SWIR/NIR$	Band Ratio SWIR/NIR
9	$Blue/NIR$	Band Ratio Blue/NIR
10	$SWIR/RED$	Band Ratio SWIR/Red
11	$Blue/Red$	Band Ratio Blue/Red
12	$SWIR - Blue$	Band Difference SWIR – Blue
13	$NIR - SWIR$	Band Difference NIR – SWIR
14	$NDVI: \frac{(NIR-Red)}{(NIR+Red)}$	NDVI (Normalized Difference Vegetation Index)
15	NDI NIR – SWIR: $\frac{(NIR-SWIR)}{(NIR+SWIR)}$	NDI (Normalized Difference Index) NIR-SWIR (also referred to as Normalized Difference Water Index – NDWI)
16	$\frac{(SWIR - Blue)}{(NIR - SWIR)}$	Ratio of the two difference images: (SWIR-Blue) / (NIR-SWIR)
17	$(Mean\ euclid.\ texture\ Blue + Mean\ euclid.\ texture\ Red + Mean\ euclid.\ texture\ NIR) / 3$	Mean of the euclidean texture bands of the Blue, Red and NIR spectral bands. The Euclidean texture band derivatives are based on the calculation of the mean euclidean texture with a moving window of 3x3 pixels applied to each Proba-V band. The mean euclidean texture per band represents the average Euclidean distance between the centre pixel and each of its 8 neighbours. The result is averaged for the blue, red, and NIR Proba-V bands.
18	$Mean\ euclid.\ texture\ Blue / Mean\ euclid.\ texture\ NIR$	Ratio of the euclidean texture of the Blue and the NIR bands
19	$Mean\ euclid.\ texture\ Blue / Mean\ euclid.\ texture\ Red$	Ratio of the euclidean texture of the Blue and the Red bands

20	<i>Mean euclid. Texture SWIR / Mean euclid. texture Red</i>	Ratio of the euclidean texture of the SWIR and the Red bands
21	<i>Mean euclid. Texture SWIR / (Mean euclid. Texture Blue + Mean euclid. texture Red + Mean euclid. texture NIR) / 3</i>	Ratio of the euclidean texture of the SWIR band and the mean of the euclidean texture bands of the Blue, Red and NIR spectral bands
22	<i>SD of (Mean euclid. Texture Blue + Mean euclid. texture Red + Mean euclid. texture NIR) / (Mean euclid. Texture Blue + Mean euclid. texture Red + Mean euclid. texture NIR) / 3</i>	Variation coefficient of the euclidean texture bands of the Blue, Red and NIR spectral bands
23	Number of Model 1 parameters 18,19,20, which amount to less than 1.5 (ranges from 1 to 3)	Number of euclidean band ratios that are smaller than 1.5
24	Average of Model 1 parameters 18,19,20	Mean of euclidean band ratios

4.1.2 *Cloud Model 1 - Part 2 - Derivation of Clouds, Haze, Snow, and Ice (undifferentiated)*

For the above described parameters thresholds were defined to derive a total of 66 classes, which are at this stage not yet separated into clouds, haze, etc., but contain all these classes. This output is referred to as **Cloud Model 1 output 04**.

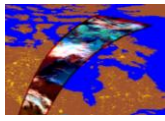
During model development, the brightest classes with the highest probability to represent clouds were defined first, followed by successively ambiguous cloud classes covering also cloud edges and haze, as well as snow and ice. The class boundaries in the individual parameters were tested and redefined in several iterations, until a high share of clouds, haze, ice and snow were covered in the different test images available. This was tested and examined in different scenes from all seasons and the entire globe.

The classes were combined starting with the most likely cloud classes, adding each additional class only to pixels that were not yet fallen into more probable classes. This way, a grouping of the resulting classes became possible according to their approximate reliability, allowing for the definition of a filtering strategy applied to these class groups, instead of treating (filtering) each cloud/haze/snow/ice class individually. Overall, this procedure resulted in 66 classes as mentioned earlier, of which especially the first 15 classes, after some noise filtering, may be regarded as a rather reliable and yet fairly complete set of clouds.

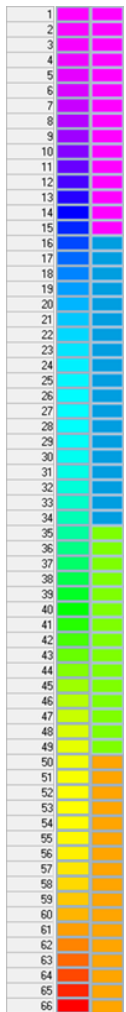
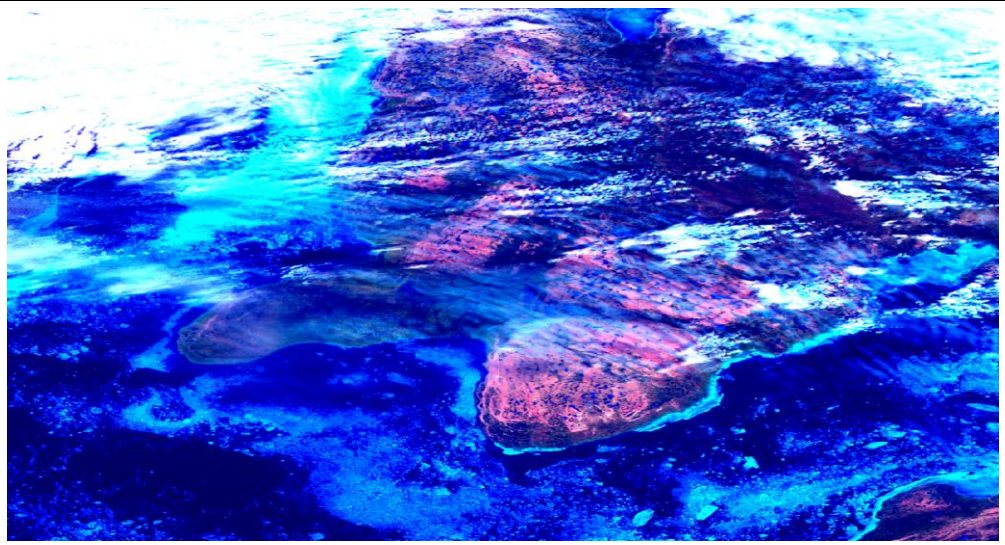
However, these 15 classes are still underrepresenting the total amount and area of clouds, haze, etc., while the other 51 classes let to a much more complete coverage, though partially at the expense of reliability. In general, the classes become roughly more unreliable with increasing class number (i.e. position in the sequential adding of classes). In addition, there are a few classes that exhibit an especially strong tendency to frequently cover unclouded or snow/ice-free areas. These classes have been intensely studied and were tried to be defined with more restrictive thresholds without losing too many valid results.

Depending on the underlying surface types and their reflectance, atmospheric conditions and the sensor and sun illumination geometry, the defined cloud classes exhibit a differentiated picture of overshooting effects: in general, vegetated surfaces show less commission errors (understood from the perspective of cloud retrieval, i.e. false clouds), while some bare areas and certain land cover types and transition zones are commonly falsely classified as cloudy areas due to their brightness and/or moisture content. Water boundaries and river valleys in particular and wetlands, often adjacent to

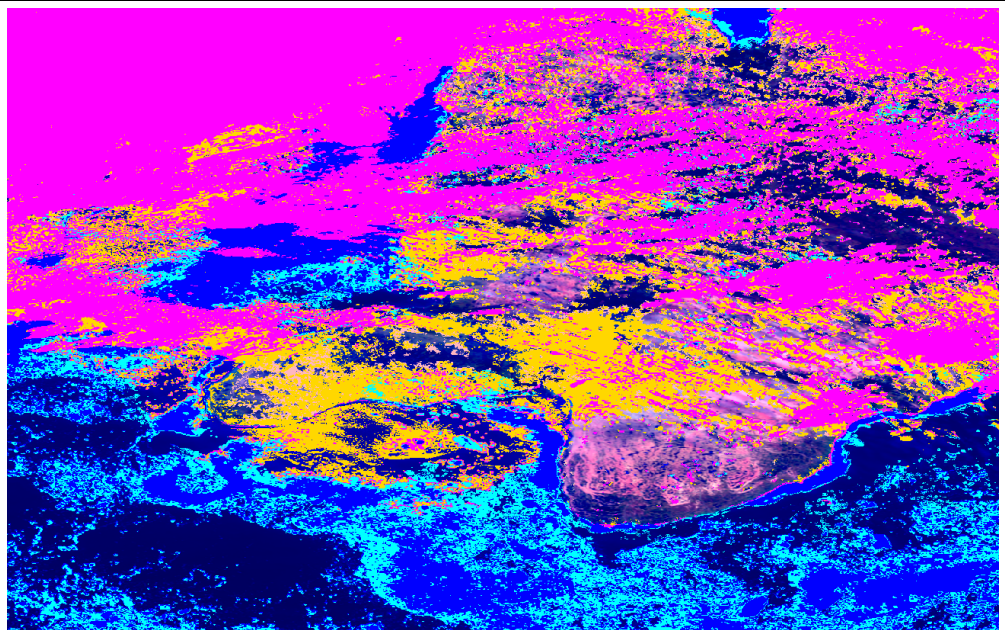
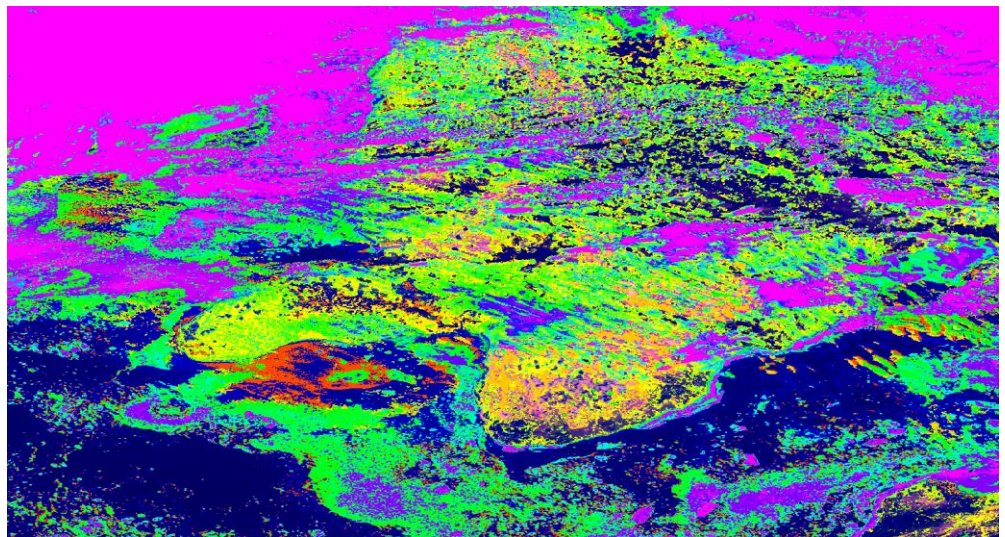
open water, as well as tidal zones and most typically salt lakes were found to be often misclassified as clouds, to some degree also agricultural areas (with their field structures), cities and smaller towns.



probav_l2a_2014
0621_174841_2_
333m_v001.img,
an image from
June 21, 2014
from northern
Canada



Color legend of
the 66 classes
(middle image)



Clouds	
Haze	
Snow and Ice	
Thin/partial snow/ice	

Final classification
result (lowest
image to the
right)

Figure 11: Example of the cloud classification result of Cloud Model 1 with 66 undifferentiated classes (that is every class may include clouds, haze, ice, or snow). The commission errors increase with the higher classes (towards yellow and reddish tones) with decreasing brightness of the features. The right hand colour bar in the middle of the left hand column refers to the class aggregation (parameter 9 in Table 2), the lowest colour legend belongs to the final result

Urban areas may indeed be often hazy, even cloudy in some pixels depending mainly on industrial, transportation related and private emission sources. The images were frequently and locally contrast optimized in order to make the haze and cloud edges visible and to minimize omission errors.

In Figure 11 a Proba-V image example is shown along with the classification result, i.e. the 66 classes derived in Cloud Model 1. The overshooting classification, as said before, was deliberately accepted in order to capture as many clouds as possible. The variety and the complex patterns of clouds, haze and here also ice can be seen in Figure 11.

4.2 Model 2 – Derivation of Image and Ancillary Parameters

The second model derives all image and ancillary parameters that are used for the filtering of the clouds, haze, ice/snow pixels and their class separation. These parameters are then used in Model 3.

In Table 2 the parameters derived in Model 2 are listed. They are calculated in this separate model in order to not overload the filtering model. The graphical version of Model 2 for parameter calculation is presented in Figure 12. The filtering approach uses partly new image parameters in relation to Model 1, which include also some parameters derived from ancillary data, i.e. CCI LC data (see Figure 13). Table 2 contains both model parameters common of Model 1 and Model 2, and new parameters only used in Model 3.

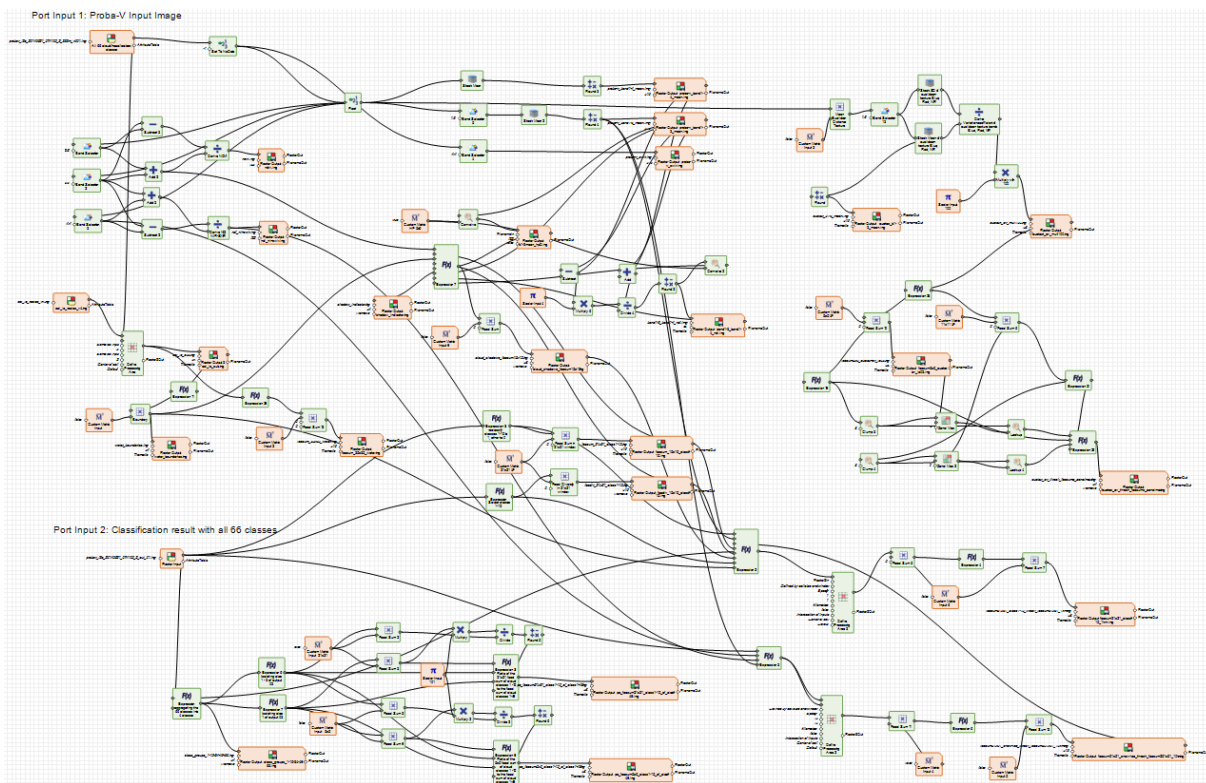


Figure 12: Model for derivation of the image and ancillary parameters used for Model 2 (filtering)

Table 2: Input parameters derived in Model 2 for usage in Model 3

No	Parameters used for filtering	Raster file name	Description
1	Proba-V bands	proba-v_blue.img proba-v_red.img proba-v_nir.img proba-v_swir.img	Proba-V image reflectance bands, helping separate clouds/haze from snow/ice.
2	Cloud Model 1 output 4 of, with filters applied: input for the filters are the Model 2 parameters 3,17,18, 19,21,24	probav_file-identification_out_01.img	66 cloud/haze/ice/snow classes, where the first 15 classes represent the most reliable cloud classes. They are filtered based on class diversity, frequency of occurrence, presence of shadow/cloud edge pixels (Model 2 parameter 13), and the presence of water boundaries.
3	$(Blue + Red + NIR)/3$	proba-v_band1-3_mean.img	Mean of Blue, Red, and NIR band
4	$(Blue + Red + NIR + SWIR)/4$	proba-v_band1-4_mean.img	Mean of Blue, Red, NIR, and SWIR band
5	NDVI: $\frac{(NIR-Red)}{(NIR+Red)}$	NDVI.img	Normalized Difference Vegetation index, assisting the reduction of commission errors.
6	NDI NIR – SWIR: $\frac{(NIR-SWIR)}{(NIR+SWIR)}$	ndi_nir-swir.img	Normalized Difference Index NIR – SWIR (also referred to as Normalized Water Index), contributing to the separation of clouds/haze and snow/ice.
7	Model 1 Input 16 (see Table 1)	euctex_b1-3_mean.img	Mean of Euclid. Texture Bands 1, 2, 3 (Blue, Red, NIR): high values are taken as indicator for the presence of clouds (e.g. > 100), but thresholds are different in different contexts.
8	Model 1 Input 21 (see Table 1)	euctext_cv_mult100.img	Variation coefficient (CV) of Euclid. Texture Bands 1, 2, 3 (Blue, Red, NIR) multiplied with 100. This parameter and its derivatives (9, 10) are used to reduce commission errors.
9	a) Maximum focal sum of thresholded (≤ 30) Model 2 Parameter 8 derived in a moving 5x5 pixel window b) Maximum focal density of thresholded (≤ 30) Model 2 Parameter 8 derived in a moving 11x11 pixel window	focsum5x5_euctex-cv_le03.img focsum11x11_euctex-cv_le03.img	After applying a threshold of 30 to Model 2 Parameter 8 and discarding values > 30, the focal sum of the remaining pixels in a 5x5 moving window is calculated. The maximum value on a segment basis is calculated. The same parameter is derived with a 11x11 moving window (discarding frequencies of less than 15 pixel), though only used for generation of Model 2 Parameter 10
10	Zonal (object based) maxima of the aggregated Model 2 Parameter 9a and 9b are determined and thresholded into two classes: class 1 is based	euctex_cv_thresh_focsums_zonal_max.img	The resulting parameter is derived by thresholding the maxima of the frequency of pixels of Model 2 parameter 9a and 9b:

	on zonal maxima of 18 (5x5 pixel window) and respectively 50 (11x11 pixel window). Class 2 is derived by applying thresholds of 6 and 30, respectively.		The two classes are used eliminate wrongly classified clouds and applied to different cloud class groups.
11	$\frac{((Blue + Red + NIR)/3 - (Blue + Red + NIR + SWIR)/4)}{((Blue + Red + NIR)/3 + (Blue + Red + NIR + SWIR)/4)}$	band1-3_band1-4_ndi.img	Normalized difference index (NDI) of Proba-V band means Blue/Red/NIR and respectively Blue/Red/NIR/SWIR. This parameter served to reduce commission errors.
12	A High Pass filter (15x15 pixel window) is applied to parameter 11, values below 100 are discarded, and for the remaining objects the respective Maximum value is determined and assigned to the entire objects.	band1-3_band1-4_ndi_hp15-ge0_zonal_max.img	This parameter enhances Parameter 11 at a local scale by enabling the extraction of high values in the local context, which may be low when looked at a the global scale.
13	High Pass filter (5x5 pixel window) applied to Model 2 Parameter 2, using a 5x5 window with a kernel centre of 24 in a matrix of -1 values	b1-3mean_hp5.img	High Pass (HP) filter applied to the mean of Proba-V bands Blue/Red/NIR, used for deriving a shadow parameter (13)
14	Ratio of the focal sum (in a 5x5 moving window) of cloud classes 1-15 (aggregated) to the focal sum (in a 5x5 moving window) of cloud classes 1-49 (aggregated)	pc_focsum5x5_class1-15_of_class1-49.img	This parameter provides a measure for the share of the most reliable cloud pixels (classes 1-15) of the classes 1-49, calculated in a moving window of 5x5 pixels.
15	Ratio of the focal sum (in a 21x21 moving window) of cloud classes 1-15 (aggregated) to the focal sum (in a 21x21 moving window) of cloud classes 1-49 (aggregated)	pc_focsum21x21_class1-15_of_class1-49.img	This parameter provides a measure for the share of the most reliable cloud pixels (classes 1-15) of the classes 1-49, calculated in a moving window of 21x21 pixels.
16	Aggregation of the 66 classes of Model 1 output 4 into 4 classes reaching from: 1-15 (class 1), 16-34 (class 2) , 35-49 (class 3), 50-66 (class 4)	class_groups_1-15-34-49-66.img	Aggregated classification result containing four classes ranging from bright/dense clouds (and snow/ice) to haze and respectively thin or partial snow cover
17	Cloud edge/shadow indicator derived with the following inputs: Model 2 Parameter 2, 11, 12, 18, 19, and 23 and a 5x5 HP filter applied to Model 2 Parameter 11. Cloud edges or shadow pixels are derived with thresholds applied to these parameters, and of the result, the focal sum	cloud_shadows_focsum15x15.img	An indicator of cloud edges or shadows respectively, whose presence/absence being is taken as partial indicator for the presence/absence of clouds

	in a moving window of 15x15 pixels is calculated		
18	Focal sum of the aggregated classes 1 – 15 of Model 1 output 4 calculated in a 15x15 pixel moving window	focsum_15x15_class1-15.img	Frequency of the aggregated classes 1-15 calculated in a 15x15 pixel window
19	Focal diversity of the aggregated classes 1 – 15 of Model 1 output 4 calculated in a 15x15 pixel moving window	focdiv_15x15_class1-15.img	Diversity (i.e. number of different classes) of the aggregated classes 1-15 calculated in a 15x15 pixel window. Class diversity is used as an indicator for the classification reliability: the higher the diversity, the more likely are the derived clouds.
20	Of the band mean of all 4 Proba-V bands values ≥ 950 are counted in a 35x35 moving window	focsum_35x35_bandmean_1-4_ge950.img	An indicator of overall brightness, showing roughly the distribution of clouds
21	Focal sum of the preliminary snow/ice pixels calculated in 2 iterations after conversion of the pixel size to 10skm. In the first iteration. At first, a 51x51 pixel moving window, then a 251x51 (columns x rows) window is used. The preliminary snow/ice pixels are derived with thresholds applied to Model 2 parameters 1, 2, 3, and 6: 1: SWIR < 280 2: belong to classes 1-66 3: ≥ 600 6: ≥ 0.45	focsum51x51_snow-ice_thresh_focsum251x51_10km.img	Frequency of preliminary ice/snow pixels calculated in 2 iterations after transforming the input raster (300m) to 10 skm pixels. This parameter represents the large-scale frequency, i.e. a preview of the larger ice/snow areas. It is used in the filtering of the safe cloud classes 1-15 (see 4.3.1) and for the treatment of snow and ice pixels.
22	Subset of reclassified classes of CCI LC: Class 0: Land surface Class 1: World oceans Class 2: Big Lakes (the great Northern American lakes) Class 3: Other water bodies > 50 pixel (à 300mx300m) Class 4: Land areas	cci_lc_sub.img	Subset of the CCI LC global land cover classification with aggregated classes separating land and water, and subdividing water into three classes (see Figure 13).
23	Using CCI Land Cover data: For large water areas, the focal sum (derived in a 35x35 pixel moving window) of water pixels is derived	focsum_35x35_water.img	Based on a mask of the world oceans and the largest lakes, the frequency of water pixels is derived in a 35x35 pixel moving window. The output is used for differentiated thresholding approaches for water, land and the larger land-water transition zones (beyond the water boundaries as derived as parameter 24.

<p>24</p>	<p>Water boundaries are derived from the CCI LC water areas (all) with a 5x5 pixel boundary filter</p>	<p>water_boundaries.img</p>	<p>Using a 5x5 pixel moving window, the inner and outer edges of water areas are derived. This mask file is used to discard assumably false clouds, as water borders often contain misclassified pixels.</p>
<p>25</p>	<p>A weighted combined parameter composed of:</p> <ul style="list-style-type: none"> • focsum_35x35_bandmean_1-4_ge950.img (20) • class_groups_1-15-34-49-66.img (16) • pc_focsum21x21_class1-15_of_class1-49.img (15) • cloud_shadows_focsum15x15.img (17) 	<p>most_likely_cloud_regions.img</p>	<p>A synthesis indicator that summarizes at a large scale the probability of the presence of clouds based on various other parameters, including overall brightness (parameter 4) and the class groups of the 66 cloud classes initially captured. It is used for adjusting the strength of some filtering steps.</p>

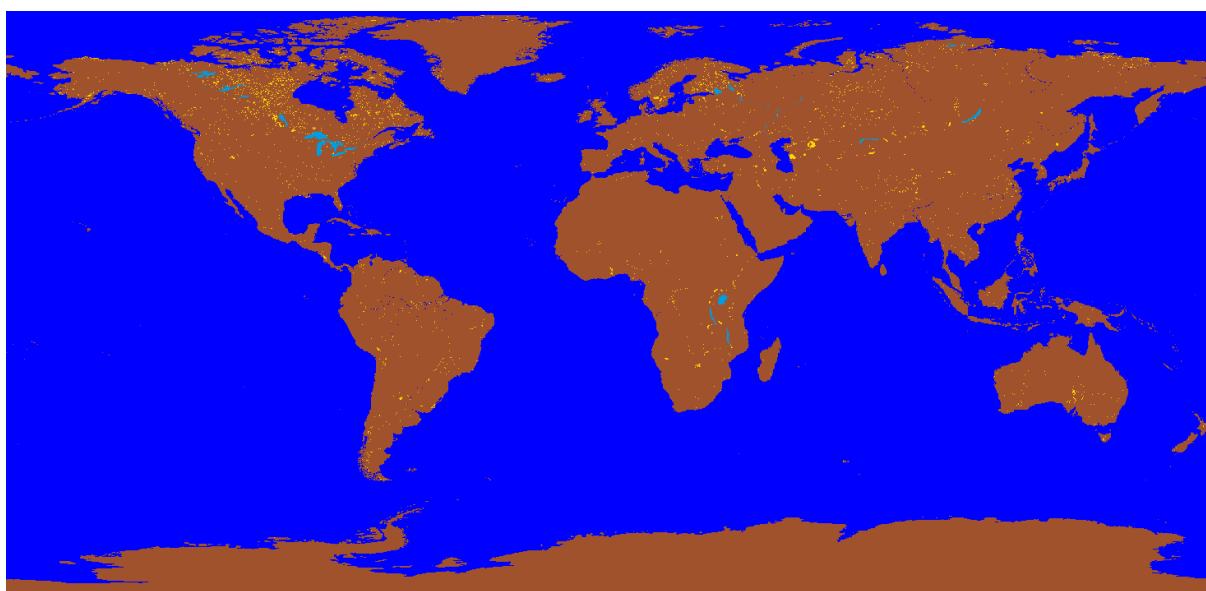


Figure 13: Reclassified CCI LC (2010) with large lakes in light blue and smaller water bodies in yellow

Figure 13 shows the reclassified CCI LC map. According to the usage of the CCI LC data, they have been adapted in the following way: The world oceans, the largest lakes and the other water bodies were separated from land. The large lakes were visually selected and comprise the lakes shown in light blue. The remaining smaller water bodies were filtered to keep only those covered by at least 50 pixels (à 300x300m²). This threshold was visually determined. Land surfaces were aggregated to one class. Water boundaries were derived for the oceans and large lakes with a 5x5 pixel moving window. These are used for discarding cloud pixels under certain further conditions as described in the next section. In addition to the water boundaries, a broader water parameter was derived (parameter 23, Table 2) in order to isolate the large and open water areas. Simply omitting the water boundaries would not have fulfilled this purpose, as the boundaries were confined to 5 pixels width.

4.3 Model 3 – Filtering and Reclassification

In the third model the still undifferentiated clouds, haze, and ice/snow pixels are filtered in order to eliminate commission errors. In addition, the third model separates clouds from haze, as well as ice/snow from clouds and haze, and finally closes gaps under certain conditions.

The filtering approach is not merely based on the object size, but uses size in combination with various further criteria. In all cases, thresholding of the input parameters is applied. Figure 14 shows the graphical model (ERDAS Imagine Spatial Model Editor) of the filtering and re-classification procedure.

Model 3 uses the 25 image parameters (i.e., raster files) generated in Model 2 (see Table 2), produces additional parameters from intermediate results and many of the parameters are input to several of the operators used. Therefore, the graphical structure of Model 2 looks somewhat complex.

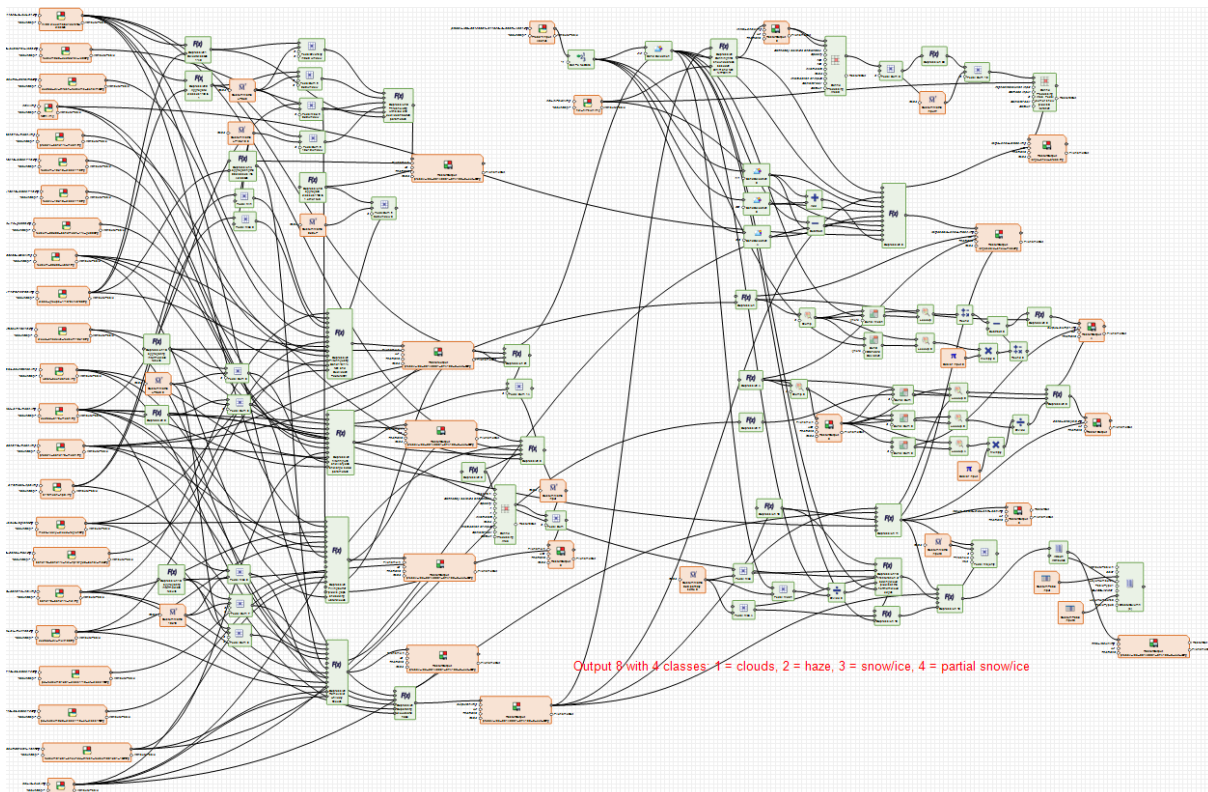


Figure 14: Overview of the second cloud processing model (ERDAS Spatial Model Editor)

In the following sections, the major operations of Model 3 are described using tables that list the input parameters, their input numbers in the ERDAS Spatial Model operators and the operations performed. These operations are exclusively thresholding functions, again (as in Model 1) with empirically determined thresholds, which are applied in various combinations and are effective in hierarchical orders. The latter means, that within an operator, the pixels occupied by the output of the first function cannot be overwritten by subsequent functions (and so on), therefore the sequence of the functions must be chosen in the most appropriate way. In several cases, temporary parameters are used for the filtering (i.e. not listed in Table 2), which are referred to as “temp” in the subsequent tables.

4.3.1 Filtering of the Safest Cloud Classes

Of the total of 66 classes produced I. Model 1, the first 15 are considered the most safe and reliable. Yet they need some filtering as they are commission errors in certain regions, especially those with bare ground and bright (snow-and ice-free) surfaces, but also along water boundaries, in some wetlands and salt lakes.

The filtering of cloud classes 1-15 is actually done in Model 2, as some further parameters are derived from the filtering results. The filtering uses 10 input parameters, four of them are only temporary raster files used in Model 2.

Table 3 lists the input parameters and filtering functions. The filtering operations use the absence/presence of shadow pixels and of water boundaries along with brightness and object size and class diversity parameters to discard part of the pixels of classes 1-15. Class diversity is an indicator for correctly classified clouds (which are very frequently composed of 10 to 20 and even more spectral classes), whereas all cloud classes tend to falsely occur on water edges. Note that class 5 is discarded more rigorously than the other classes, as it tends to scatter falsely more than the other classes. Further on, all 15 classes are kept within the preliminary snow/ice areas (Parameter 21), where they behave somewhat differently than in (snow-and ice-free) regions.

Table 3: Filtering classes 1-15

Parameter number (see Table 2)	Raster file name	Input number for operator in Spatial Model	Thresholding Functions defined in Spatial Model Operator (parameters are expressed with their input numbers listed in column 3)
18	focsum_15x15_class1-15.img	1	Conditional { (\$Input6 ge 1) \$Input7, (\$Input7 eq 1 and \$input1 ge 120) \$Input7, (\$input1 lt 100 and \$input2 eq 1 and \$Input3 eq 0 and \$Input8 eq 5) 0, (\$Input7 eq 1 and \$input1 le 30 and \$Input2 le 2 and \$Input3 eq 0) 0, (\$Input7 eq 1 and \$Input1 le 10 and \$Input2 eq 1 and \$Input3 ge 10) 0, (\$Input7 eq 1 and \$Input1 le 20 and \$Input3 eq 0 and \$Input4 eq 1) 0, (\$Input7 eq 1 and \$Input9 le 3 and \$Input10 eq 0) 0, (default) \$Input7 }
19	focdiv_15x15_class1-15.img	2	
17	cloud_shadows_focsum15x15.img	3	
24	water_boundaries.img	4	
3	proba-v_band1-3_mean.img	5	
21	focsum51x51_snow-ice_thresh_focsum251x51_10km.img	6	
temp	Aggregated classes 1-15	7	
temp	Selected classes 1-15	8	
temp	Focal sum (5x5 pixel moving window) of classes 1-15	9	
temp	Focal sum (5x5 pixel moving window) of classes 1-34	10	
Output of operation: intermediate raster file with the classes 1-15 aggregated to code 1			

4.3.2 Filtering of Classes 1 - 49

The filtering of the classes 1-49 is done in Model 3, along with all other operations described below. In Table 4 the filtering operations applied to the classes 1-49 are described. Classes 50-66 are not included

here, as they cover large areas containing often more commission errors than true clouds or especially haze. These classes are taken care of in later filtering steps. Classes 1-49 are filtered using size and class diversity criteria along with Euclidean texture parameters. High values (e.g. 50 and higher) of the Euclidean texture parameter 7 (euctex_b1-3_mean.img) are in most cases typical for clouds (though also for all other sharply contrasting edges), whereas low values of texture parameter focsum5x5_euctex-cv_le03.img (Model 2 parameter 9, derived from euctext_cv_mult100.img) are most commonly found for small clouds, cloud edges and haze. An example is shown in Figure 15, where especially the small cloud fields can be seen to contrast clearly to the background due to their low values in euctext_cv_mult100.img.

Table 4: Filtering classes 1-49

Parameter number (see Table 2)	Raster file name	Input number for operator in Spatial Model	Thresholding Functions defined in Spatial Model Operator (parameters are expressed with their input numbers listed in column 3)
temp	Classes 1-49*	1	Conditional { (\$Input2 eq 1 and \$Input3 le 12 and \$Input4 le 25 and \$Input5 le 120) 0, (\$Input2 eq 1 and \$Input3 le 12 and \$Input6 le 5 and \$Input5 le 120) 0, (\$Input3 le 7 and \$Input4 le 25 and \$Input5 le 120) 0, (\$Input3 le 7 and \$Input6 le 5 and \$Input5 le 120) 0, (\$Input1 ge 1) \$Input1, (default) 0 }
temp	focal diversity in 5x5 pixel moving window of classes 1-49*	2	
temp	focal sum in 5x5 pixel moving window of aggregated classes 1-49*	3	
temp	Focal Max in 5x5 pixel moving window of euctex_b1-3_mean.img (parameter 7 of Model 2)	4	
temp	focal sum in 15x15 pixel moving window of aggregated classes 1-49*	5	
9	focsum5x5_euctex-cv_le03.img	6	
Output 02: intermediate raster file containing the class 1 to 49 of the original 66 classes			

*Note that for the classes 1-15 only the remaining pixels after the first filtering step described in 4.3.1 are included

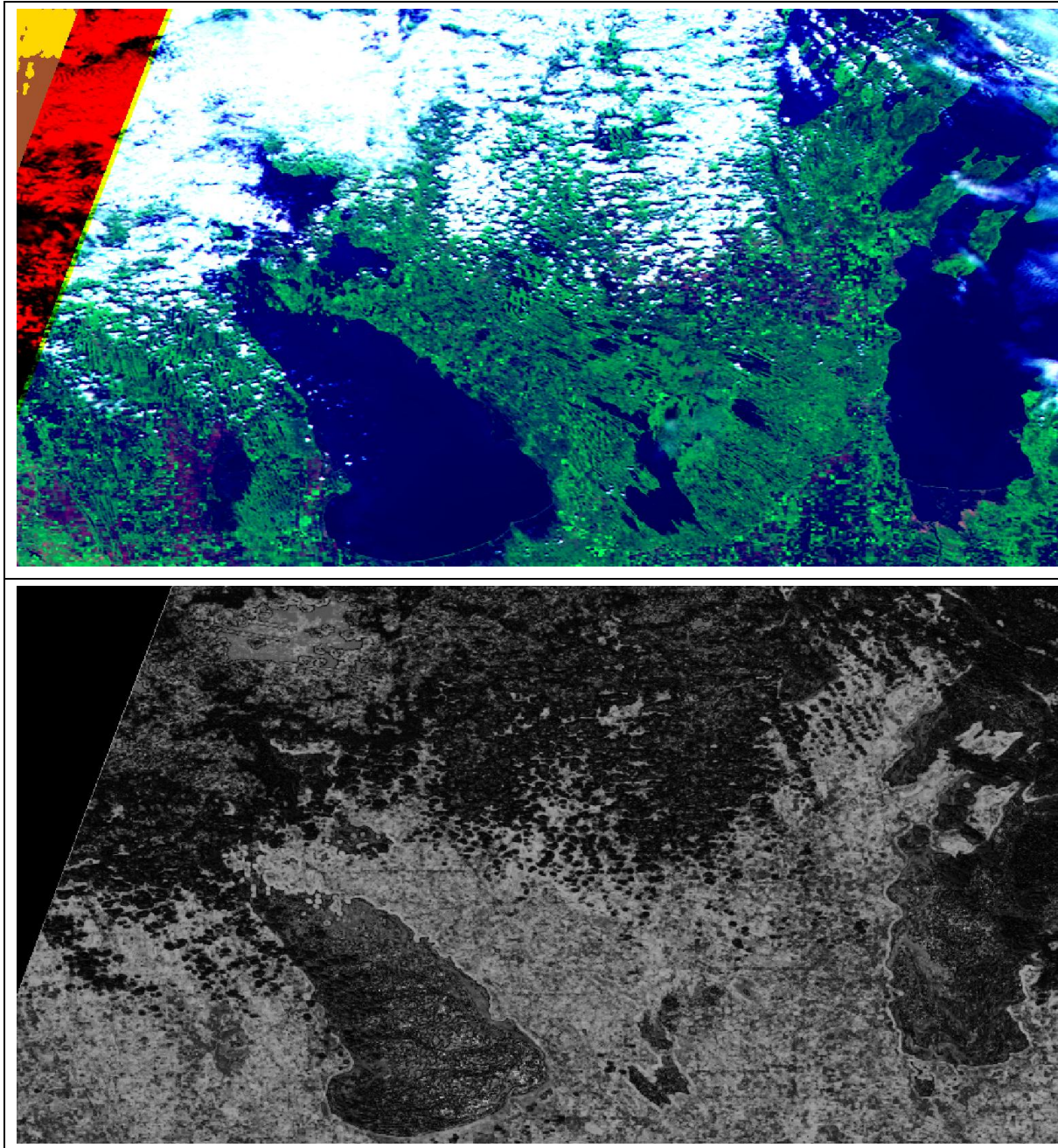


Figure 15: Central part of image probav_l2a_20140621_174841_2_333m_v001.img (SWIR-NIR-Blue RGB) with image parameter euctext_cv_mult100.img (no. 8 in Table 2) in the lower image. Haze and small clouds have very low values and can be readily enhanced with this image parameter

4.3.3 Filtering based on NDI of spectral band means and on Euclidean texture

The third filtering step uses essentially the parameter band1-3_band1-4_ndi.img (parameter 11 in Table 2 and image parameter derived from the Euclidean texture (parameter 8). The Normalised Difference Index of the spectral band means (1,2,3 and respectively 1,2,3,4) typically exhibits low (usually negative) values for unclouded areas, and higher (yet partly negative) values for clouds and often somewhat higher values for snow/ice. Like all other parameters, it is not perfect and provisions for exceptions need to be made. In this case, the first three thresholding statements in Table 5 are such provisions, which allow certain cloud classes to be included based on additional criteria, not

applying the general threshold to band1-3_band1-4_ndi.img (-2 and respectively -3), but lower thresholds instead (allowing for more cloud pixels to be included).

In addition, this filtering operation makes use of the fact that the coefficient of variation, derived for the Euclidean texture bands of Proba-V bands 1,2, and 3 (Blue, Red, NIR) was found to be an excellent parameter for the detection and respectively exclusion of haze, thin clouds, and cloud edges (see Figure 15). Nevertheless, as all others, also this parameter needs to be used carefully, i.e. with adaptations and in a differentiated way.

As described in Table 2 for Parameter 10 used in this operation, it results from two processing steps applied to Parameter 8 using two different moving window sizes (5x5 and respectively 11x11 pixels). First, euctext_cv_mult100.img is thresholded to keep only values below 30, which are aggregated to value 1. The cited moving windows are applied to the result, determining the frequencies of these pixels in the windows (focal sum). For the image objects built by these pixels (contagious cloud pixel groups), the object based maxima of frequencies are determined to serve as indicator for the presence of haze and thin clouds. The higher the frequency maximum within each cloud object, the higher is the probability that the considered object actually is a cloud or haze. The maxima are thresholded to receive two classes: class 1 is based on zonal maxima of 18 (5x5 pixel window) and respectively 50 (11x11 pixel window). Class 2 is derived by applying thresholds of 6 and 30, respectively. As can be seen in Table 5, higher frequency (Max) thresholds are applied to the aggregated cloud classes 3 and 4, which are less likely and have been observed to be correct, if they have high frequencies of low values in euctext_cv_mult100.img.

Table 5: Filtering based on NDI of spectral band means and on Euclidean texture

Parameter number (see Table 2)	Raster file name	Input number for operator in Spatial Model	Thresholding Functions defined in Spatial Model Operator (parameters are expressed with their input numbers listed in column 3)
16	class_groups_1-15-34-49-66.img	1	Conditional { (\$Input2 ge -5 and \$Input3 ge 1 and \$Input6 le -1700 and \$Input7 ge 1700 and \$Input9 ge 1 and \$input9 le 10 and \$input10 ge 1 and \$Input11 ge 370) \$Input1, (\$Input2 ge -6 and \$Input3 ge 1 and \$Input3 le 55 and \$Input4 ge 400 and \$Input5 ge 0.25 and \$Input8 le 45 and \$Input10 eq 1) \$Input1, (\$input2 ge -6 and \$input10 eq 1 and \$Input11 ge 400 and \$Input12 eq 0 and \$Input13 ge 100) \$input1, (\$Input2 le -1 and \$Input3 ge 51) 0, (\$Input2 le -3 and \$Input3 ge 18) 0, (\$Input2 le -3 and (\$Input3 eq 3 or \$Input3 eq 5)) 0, (\$Input1 eq 4 and \$Input8 ge 45) 0, (\$Input1 le 2 and \$Input10 ge 1) \$Input1,
11	band1-3_band1-4_ndi.img	2	
1	Output 04 of Model 1 (66 cloud classes)	3	
3	proba-v_band1-4_mean.img	4	
5	NDVI	5	
temp	focal Min in 15x15 pixel moving window of b1-3mean_hp5.img	6	
temp	focal Max in 15x15 pixel moving window of b1-3mean_hp5.img	7	
8	euctext_cv_mult100.img	8	
temp	focal sum in 5x5 pixel moving window of classes 1-25	9	
10	euctex_cv_thresh_focsums_zonalmax.img	10	
25	band1-3_band1-4_ndi_hp15-ge0_zonal_max.img	11	
23	focsum_35x35_water.img	12	

25	most_likely_cloud_regions.img		
Output 03: intermediate raster file with 4 aggregated classes (class aggregation as in Model 2 parameter 16)			

4.3.4 Removing false clouds using large scale filters and ancillary information

In this filtering step, large scale image parameters as well as the derived CCI LC based information are used to eliminate certain commission errors that typically occur along water edges, small lakes and dried out lakes in dry areas. Especially the latter, however cannot be completely removed without other approaches such as multitemporal methods, where data taken within short intervals can be compared to detect changes (i.e., clouds).

Table 6: Removing false clouds based on large scale parameters and ancillary information

Parameter number (see Table 2)	Raster file name	Input number for operator in Spatial Model	Thresholding Functions defined in Spatial Model Operator (parameters are expressed with their input numbers listed in column 3)
Output 02	Output 03 (outcome of previous step)	1	Conditional { (\$Input1 ge 1 and \$Input2 le 0.25 and \$Input3 le 400 and \$Input4 eq 0 and \$Input5 ge 550 and \$Input7 le 3 and \$input9 eq 0 and \$Input10 le 150 and \$Input12 lt 1000) 0, (\$Input1 ge 1 and \$Input2 le 0.25 and \$Input3 le 400 and \$Input4 eq 0 and \$Input5 ge 550 and \$Input6 eq 1 and \$input9 eq 0 and \$Input7 le 3 and \$Input12 lt 1000) 0, (\$Input1 ge 1 and \$Input3 le 400 and \$Input4 eq 0 and \$Input6 eq 1 and \$input8 le 15 and \$Input2 le 0.25 and \$Input7 le 3) 0, (\$input5 ge 550 and \$input5 le 1224 and \$Input11 le 5) 0, (default) \$Input1 }
5	NDVI	2	
26	focsum_35x35_swir-le350_b1-3mean-ge400_class1-46.img	3	
17	cloud_shadows_focsum15x15.img	4	
23	focsum_35x35_water.img	5	
24	water_boundaries.img	6	
19	focdiv_15x15_class1-15.img	7	
temp	focal sum in 5x5 pixel moving window applied to aggregated output of the previous operation	8	
20	focsum_35x35_bandmean_1-4_ge950.img	9	
18	focsum_15x15_class1-15.img	10	
7	euctex_b1-3_mean.img	11	
21	focsum51x51_snow-ice_thresh_focsum251x51_10km.img	12	
Output 04: intermediate raster file with 4 aggregated classes (class aggregation as in Model 2 parameter 16)			

4.3.5 Filling buffer pixels and gaps and adding clouds over water

This operator essentially fills gaps and buffer regions of the so far established clouds using two different buffer sizes and within these buffers different distance thresholds. Cloud pixels taken from the original classification result are filled in, if they fulfil the criteria given by the other, thresholded input parameters. In addition, clouds over water are added, both using the classified pixels out of the 66 original classes and additional pixels fulfilling the defined criteria.

Table 7: Filling buffer pixels and gaps and retrieving more clouds over water

Parameter number (see Table 2)	Raster file name	Input number for operator in Spatial Model	Thresholding Functions defined in Spatial Model Operator (parameters are expressed with their input numbers listed in column 3)
25	most_likely_cloud_regions.img	1	Conditional { (\$Input1 ge 200 and \$Input2 ge 1 and \$Input2 le 46 and \$Input3 ge -1 and \$input4 ge 450 and \$input6 le 30 and \$input8 ne 1) 1, (\$Input1 ge 200 and \$Input2 ge 1 and \$Input2 le 46 and \$Input3 ge -1 and \$input4 ge 600 and \$Input5 ge 35 and \$input6 le 50 and \$input8 ne 1) 2, (\$input1 ge 100 and \$input2 ge 1 and \$input2 le 46 and \$input7 le 10 and \$input13 ge 100) 3, (\$input3 ge -1 and \$input4 ge 450 and \$input7 ge 17 and \$input11 eq 0) 4, (\$input7 ge 23 and \$input11 eq 0) 5, (\$input1 ge 200 and \$Input9 ge 10) 6, (\$input1 ge 200 and \$Input10 ge 10) 7, (\$input1 ge 200 and \$input14 ge 3 and \$input15 ge 1 and \$input15 le 3 and \$Input16 ge 1 and \$input16 le 400) 8, (\$input2 ge 1 and \$input3 ge -4 and \$input3 le 10 and \$input5 ge 10 and \$input12 ge 1100 and \$Input14 ge 1 and \$Input14 le 2) 10, (\$input2 ge 1 and \$input3 ge -4 and \$input3 le 10 and \$input5 ge 10 and \$input12 ge 750 and \$input12 le 1224 and \$Input14 ge 1 and \$Input14 le 2 and \$Input16 ge 1 and \$Input16 le 400 and \$Input8 eq 0) 11, (\$input3 ge -2 and \$input3 le 10 and \$Input5 ge 25 and \$input12 ge 1100 and \$Input14 ge 1 and \$Input14 le 2) 12, (\$input3 ge -2 and \$input3 le 10 and \$Input5 ge 25 and \$input12 ge 750 and \$input12 le 1224 and \$Input14 ge 1 and \$Input14 le 2 and \$Input16 ge 1 and \$Input16 le 400) 13, (\$input4 ge 400 and \$input5 ge 5 and \$input12 ge 750 and \$input12 le 1224 and \$Input14 ge 1 and \$Input14 le 2 and \$input16 ge 1 and \$input16 le 400) 14, (\$input4 ge 400 and \$input12 eq 1225 and \$Input14 ge 1 and \$Input14 le 2 and \$input16 ge 1 and \$input16 le 400) 15, (default) \$input11}
2	Output 4 of Model 1 containing the original 66 classes	2	
11	band1-3_band1-4_ndi.img	3	
3	proba-v_band1-3_mean.img	4	
7	euctex_b1-3_mean.img	5	
8	euctext_cv_mult100.img	6	
temp	focal sum in 5x5 pixel moving window applied to aggregated output 04	7	
24	water_boundaries.img	8	
15	pc_focsum21x21_class1-15_of_class1-49.img	9	
14	pc_focsum5x5_class1-15_of_class1-49.img	10	
Intermediate output	Output 04 (outcome of previous step)	11	
23	focsum_35x35_water.img	12	
temp	Focal Max in 5x5 pixel moving window applied to euctex_b1-3_mean.img (input 5)	13	
22	cci_lc_sub.img	14	
Intermediate output	Output 03	15	
temp	Large scale cloud gaps (1km pixel size, 21x21 pixel moving window)	16	

Output 05: intermediate raster file with differentiated class codes enabling to trace back the changes made. Code 10 to 15 are used for added clouds over water.

The addition of clouds over water areas is considered of advantage to derive a more complete cloud map over water areas, as the filtering steps applied so far do remove some cloud pixels (in as much as water is not taken out from the filtering), but mainly because the original 66 classes do sometimes not capture clouds over water completely. Especially mixed cloud pixels over water and thin clouds tend to have low reflectance values that it was preferred to introduce these cloud pixels only in the filtering operations under control of the water mask and the derived parameters. An important parameter in this context is the Euclidean texture (parameter 7), which is typically and very consistently higher for clouds over water than for cloud free water. Part of the clouds, which have not been captured in the 66 class output of Model 1 have been retrieved this way. In addition, a brightness parameter, i.e. the Proba-V mean of bands 1,2, and 3 (parameter 3 in Table 2) is used as additional criterion for including further clouds pixels over water areas and within cloud gaps (over land and water).

The accepted and added cloud pixels resulting from this operation are numbered from 1 to 15 (leaving out code 9), where the codes from 10 onwards belong to the added cloud pixels over water. The latter have been added using parameter `focsum_35x35_water.img` with different thresholds: as this parameter contains the number of water pixels (oceans and big lakes derived from CCI LC, see 4.2) derived in a 35x35 moving window, a threshold of 1225 (= 35x35) means that the respective operation is only applied to open water pixels without land pixels in their larger neighbourhood. In the case of large water bodies a threshold of 750 means that the coastlines are not included, but the water areas close to the coast (and narrow water bodies with low values in `focsum_35x35_water.img`) are also excluded. The temporary input parameter 16 (large scale cloud gaps derived in 1km pixel size, 21x21 pixel moving window) is introduced to define areas (in combination with `focsum_35x35_water.img`) close to the coasts with a high large scale cloud density, in order to add back clouds over water boundaries that have been filtered away previously by using the water boundary parameter.

Figure 16 shows an example of added clouds over water in the southern part of Proba-V image `probav_l2a_20140921_053508_3_333m_v001.tif`. The footprint image in the upper right shows the location west of India in the white little rectangle with the classification result superimposed. The Proba-V is depicted in band combination SWIR-NIR-Blue (RGB), with a “normal” contrast stretch adapted to the land area in the region. Accordingly, only the brighter clouds can be seen, and only these are captured in the initial classification result (output of Model 1 with 66 classes). This may be acceptable for land applications, however for water mapping purposes, even faint clouds will corrupt the data due to the small signal to noise ratio of the water reflectance. The proposed method can facilitate the retrieval of such faint clouds and of mixed cloud-water pixels.

Different thresholds are applied to the Euclidean texture image for the cloud retrieval, depending on the values of the other parameters used, as can be traced back in Table 7.

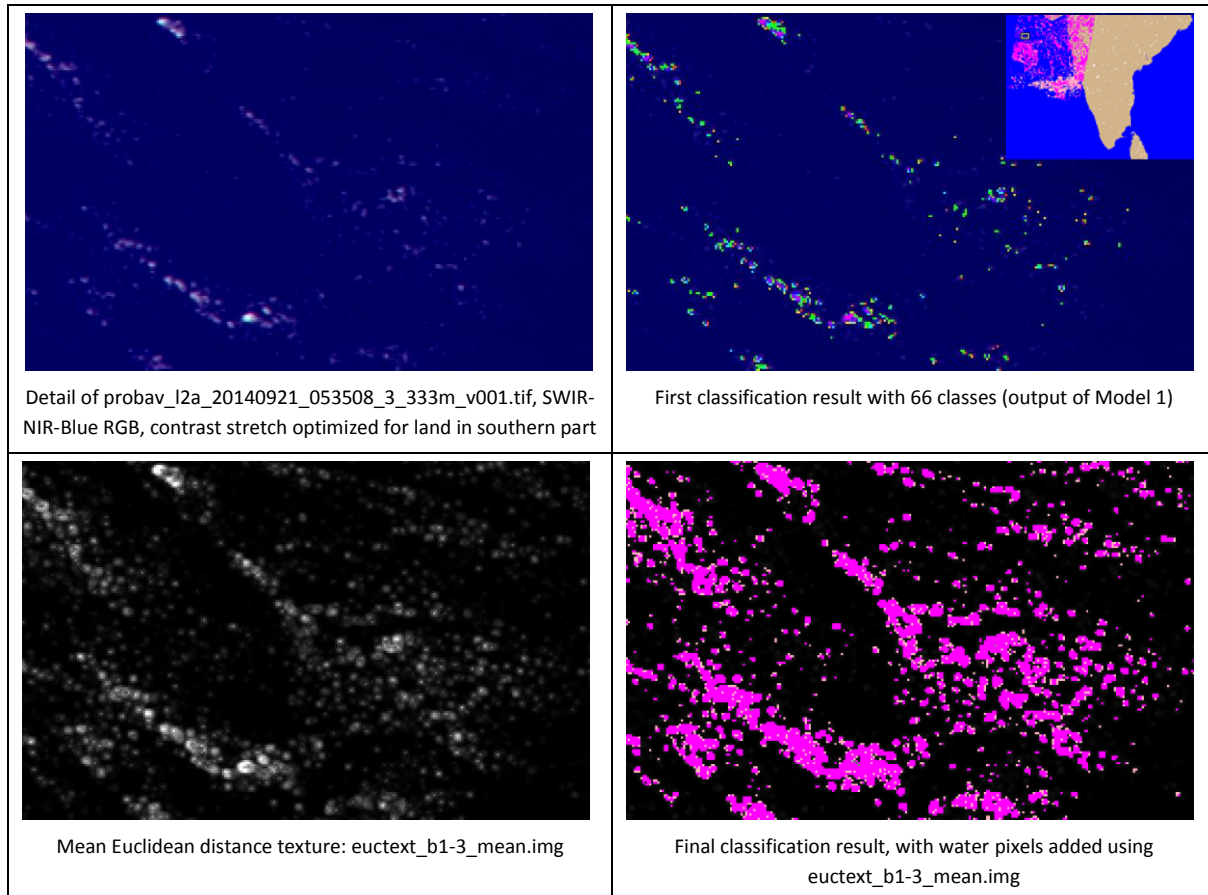


Figure 16: Comparison of first classification result of clouds over water to final result after adding water based on the mean euclidean distance texture parameter

4.3.6 Final cloud filtering

The final filtering step removes unlikely clouds based on large scale masks of the major cloud and haze areas, on the presence of shadow indicator pixels, Euclidean texture parameters, the band mean NDI of Proba-V bands 1-3 and respectively 1-4 (parameter 11), on the original class (out of the 66 classes, here represented in the aggregated parameter 16), on the quantity of cloud pixels, and on ancillary data, i.e. the water boundaries (based on CCI LC data 2010, see Parameter 24 in Table 2). Again, object size criteria (input 5) are always combined with other criteria in order to keep as many likely small clouds as possible. Table 8 summarizes inputs and the thresholding functions.

Table 8: Removal of Unlikely Clouds

Parameter number (see Table 2)	Raster file name	Input number for operator in Spatial Model	Thresholding Functions defined in Spatial Model Operator (parameters are expressed with their input numbers listed in column 3)
Intermediate output	Output 05	1	Conditional { (\$Input5 le 50 and \$Input6 eq 0 and \$Input7 eq 1) 0,
16	class_groups_1-15-34-49-66.img	2	
25	most_likely_cloud_regions.img	3	

temp	Focal Max (15x15 pixel moving window) of euctex_b1-3_mean.img (Parameter 7)	4	(\$Input12 le 15 and \$Input6 eq 0 and \$Input7 eq 1) 0, (\$input1 ge 10) 5, (\$input2 eq 4 and \$input3 eq 0 and \$input4 le 20 and \$input5 le 20) 0, (\$input5 le 20 and \$input8 le -6 and \$input9 ge 35 and \$input11 gt 1000) 0, (\$Input3 eq 0 and \$Input4 le 100 and \$Input5 le 100 and \$Input6 eq 0 and \$Input10 ge 3) 0, (\$Input1 ge 1) \$Input1, (default) 0 }
temp	focal sum in 15x15 pixel moving window applied to aggregated output 05	5	
17	cloud_shadows_focsum15x15.img	6	
24	water_boundaries.img	7	
11	band1-3_band1-4_ndi.img	8	
8	euctext_cv_mult100.img	9	
22	cci_lc_sub.img	10	
21	focsum51x51_snow-ice_thresh_focsum251x51_10km.img	11	
Output 06: same coding as Output 05			

4.3.7 Separation of clouds and haze

The separation of clouds and haze is based on brightness and texture parameters, the band mean NDI of Proba-V bands 1-3 and respectively 1-4, and on the original class (1-66) derived in model 1. The assumptions and the observations here are basically that brighter clouds with stronger textures and higher band mean NDI (parameter 11) tend to be more likely clouds, and the opposite applies to haze. Table 9 summarizes inputs and the thresholding functions, and Figure 17 shows an example on a result.

Table 9: Separation of clouds and haze

Parameter number (see Table 2)	Raster file name	Input number for operator in Spatial Model	Thresholding Functions defined in Spatial Model Operator (parameters are expressed with their input numbers listed in column 3)
Intermediate output	Output 06	1	Conditional { (\$input1 ge 1 and \$input2 le 17 and \$input3 ge 7 and \$input4 ge 600 and \$input6 ge 5) 1, (\$Input1 ge 1 and \$Input2 ge 47) 2, (\$Input1 ge 1 and \$Input3 le 7 and \$Input4 le 700) 2, (\$Input1 ge 1 and \$Input2 le 17 and (\$Input3 ge 30 or \$Input4 ge 800)) 1, (\$Input1 ge 1 and \$Input2 le 46 and \$Input5 ge 1500) 1, (\$Input1 ge 1 and \$Input2 ge 18 and \$Input2 le 46 and \$Input3 ge 30) 1, (\$Input1 ge 1) 2, (default) 0 }
1	Output 4 of Model 1 containing the original 66 classes	2	
7	euctex_b1-3_mean.img	3	
3	proba-v_band1-3_mean.img	4	
13	b1-3mean_hp5.img	5	
11	band1-3_band1-4_ndi.img	6	
Output 07: class1 = clouds, class2 = haze			

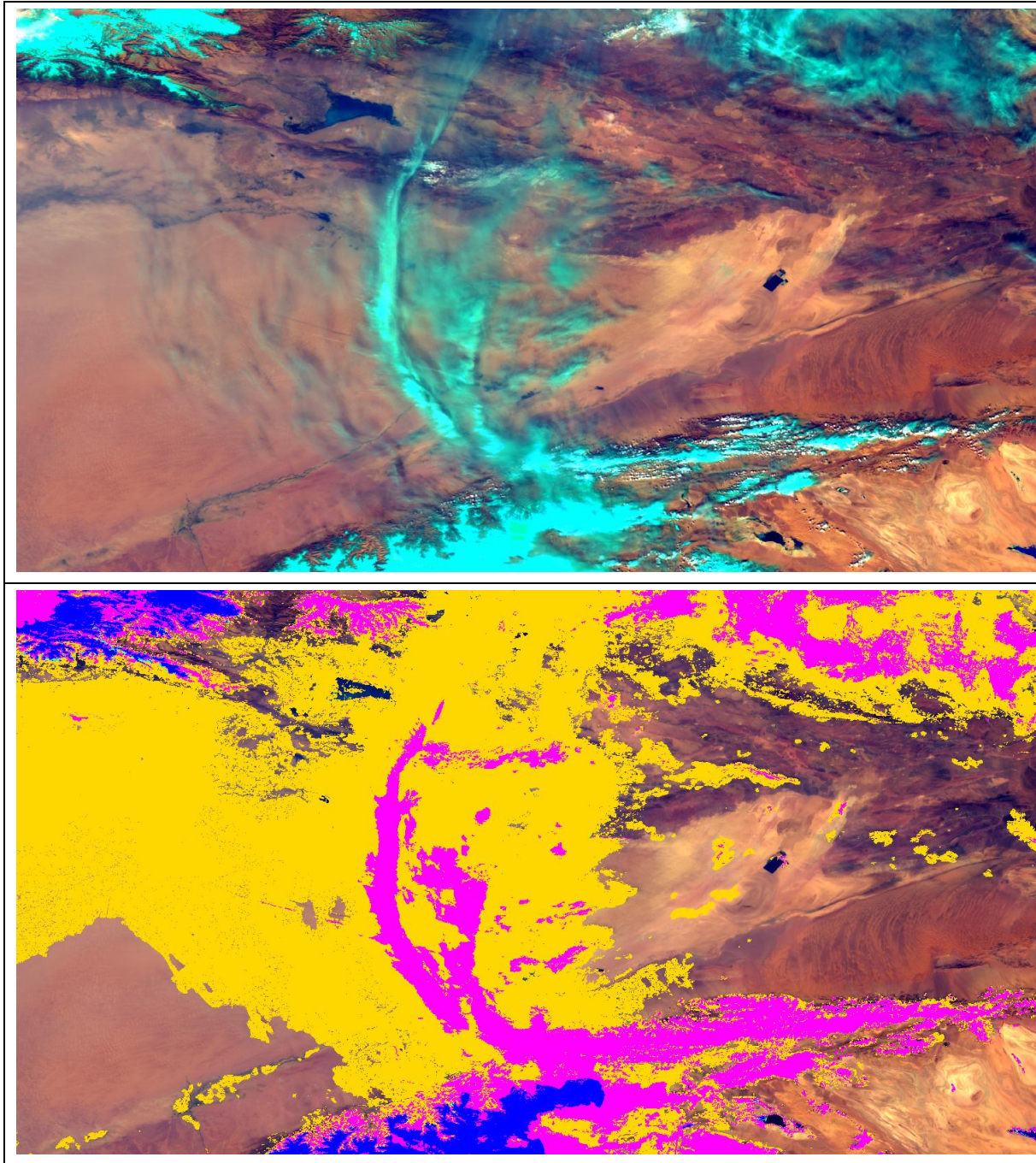


Figure 17: Differentiation of clouds (magenta) and haze (yellow) (probav_l2a_20140321_044105_3_333m_v001.img)

While the approach works partly quite well as can be seen in Figure 17, there is a tendency that part of the haze may be rather assigned to clouds. This assignment needs a lot of testing and is also subject to different definitions of what actually constitutes a cloud, and what can still be regarded as haze. When taking partial transparency of haze as criterion, this will lead to different visual interpretations in concrete situations (very much depending on the degree of contrast stretching of the image), and also with regard to reflectance properties measured by the sensor, as haze is always a mixture of ground and cloud reflectances. The assignment of haze or clouds depend also on the application, where for instance the NDVI is less sensitive to haze than other indices, therefore for NDVI calculations, some haze may still be acceptable. Therefore, the strategy followed in this algorithm was to aim at a complete and correct as possible cloud AND haze retrieval, so that the derived cloud/haze pixels can

be flexibly separated depending on the intended usage of the cloud/haze mask. In Figure 18 another example for the separation of clouds and haze can be seen.

4.4 Separation of ice and snow from clouds and haze

As mentioned earlier, snow and ice are not separated from clouds and haze from the beginning, i.e. in Model 1. Instead, the first model aims at retrieving all clouds, haze, snow and ice areas without differentiation, leading in many areas to strongly overshooting classification results, which are being filtered, thinned out, and eventually reclassified into clouds, haze, snow and ice.

In addition to the requested snow/ice class, a second snow/ice class (class number 3 in the finale result), with values in the blue band below 600, exhibiting areas with partial or thin snow cover, forests, and other areas with a greater share of ground reflectance than of those with a dense snow or ice cover. Vice versa, bright and predominantly pure snow pixels are assigned a separate class (class number 3 in the finale result).

4.4.1 Derivation of an initial snow and ice mask

Like the entire filtering steps, the separation of snow and ice from clouds and haze in this algorithm is also an iterative procedure. It starts with thresholds applied to the SWIR band and the NDI of NIR and SWIR (parameter 6 in Table 2), leading to a preliminary estimation of snow and ice areas. It is deliberately a conservative first thresholding to avoid overly large confusion errors with ice-clouds, which are easily mixed up with snow and ice areas on the basis of pixel reflectance and the indices used. The strategy in the next steps is to add snow by reclassifying probable snow areas in the in the larger vicinity of these first snow/ice areas. Table 10 shows the parameters and thresholds applied in the first snow retrieval step. Only two parameters, i.e. SWIR and the NIR-SWIR NDI are used. Tests were also performed with the parameter `band1-3_band1-4_ndi.img` (Parameter 11 in Table 2, which accomplishes a rather consistent separation of ice-clouds and surface ice/snow. However, this parameter is somewhat less sensitive for the detection of snow than the NIR-SWIR NDI, and small ice/snow patches (i.e., mixed pixels) may not be captured with this parameter. Therefore, the NIR-SWIR NDI (Parameter 6 in Table 2) was used for deriving the initial snow/ice mask, while `band1-3_band1-4_ndi.img` is better suited for deriving a large scale snow/ice mask.

Table 10: First step of snow and ice retrieval

Parameter number (see Table 2)	Raster file name	Input number for operator in Spatial Model	Thresholding Functions defined in Spatial Model Operator (parameters are expressed with their input numbers listed in column 3)
Intermediate output	Output 07	1	Conditional { (\$Input1 ge 1 and \$Input2 le 280 and \$Input3 ge 0.55) 1, (default) 0 }
1	Proba-V SWIR band	2	
6	<code>ndi_nir-swir.img</code>	3	
Output: initial snow/ice mask			

4.4.2 Reclassifying snow/ice at a large scale

In the second step of the snow/ice reclassification procedure, large scale snow/ice regions are derived and within them, further snow/ice areas are retrieved, applying additional criteria as compared to the initial snow/ice retrieval step.

The large snow and ice areas are determined by subsampling the intermediate result to 100x100 km² pixels and deriving the focal number of snow/ice pixels within a 51x51 pixel moving window applied at this reduced pixel size in two iterations. The parameters used and the thresholding functions applied within these large-scale snow regions are listed in Table 11.

Table 11: Reclassifying snow and ice in large area buffers

Parameter number (see Table 2)	Raster file name	Input number for operator in Spatial Model	Thresholding Functions defined in Spatial Model Operator (parameters are expressed with their input numbers listed in column 3)
Intermediate output	Output 07	1	Conditional { (\$Input2 ge 500 and \$Input12 eq 1) 3, (\$Input1 eq 0 and \$Input2 ge 500 and \$Input3 le 150 and \$Input5 ge 350 and \$Input6 ge 250 and \$Input10 ge 150 and \$Input11 eq 3) 3, (\$Input2 ge 500 and \$Input8 lt 750 and \$Input11 eq 4) 0, (\$Input2 ge 500 and \$Input6 lt 300 and \$Input7 ge 0.22) 0, (\$Input2 ge 500 and \$Input3 ge 360 and \$Input4 lt 0 and \$Input5 lt 350 and \$Input6 lt 340 and \$Input7 ge 0.1 and \$Input11 eq 4) 0, (\$Input1 eq 0 and \$Input2 ge 500 and \$Input3 le 280 and \$Input4 ge 0.4 and \$Input8 ge 750) 3, (\$Input1 ge 1 and \$Input2 ge 500 and \$Input3 le 280 and \$Input4 ge 0.3 and \$Input5 ge 600) 3, (\$Input1 ge 1 and \$Input2 ge 500 and \$Input3 le 380 and (\$Input5 ge 360 or \$Input6 ge 350) and \$Input4 ge 0 and \$Input5 le 600 and \$Input9 le -20 and \$Input7 le 0.05 and \$Input11 eq 4) 3, (\$Input1 ge 1 and \$Input2 ge 500 and \$Input3 le 420 and (\$Input5 ge 420 or \$Input6 ge 400) and \$Input4 ge 0.2 and \$Input5 le 650 and \$Input9 le -80 and \$Input7 le 0.2 and \$Input11 eq 4) 3, (\$Input1 ge 1 and \$Input2 ge 500 and \$Input3 le 360 and \$Input4 ge 0.3 and \$Input11 ge 3) 3,
temp	Large area snow mask	2	
1	Proba-V SWIR band	3	
6	Ndi_nir-swir.img	4	
1	Proba-V Blue band	5	
1	Proba-V Red band	6	
5	NDVI.img	7	
temp	Sum: Proba-V Blue band + Proba-V Red band	8	
temp	Difference SWIR - Blue	9	
1	Proba-V NIR band	10	
22	Cci_lc_sub.img	11	
Intermediate output	Initial snow/ice mask	12	

			<pre> (\$Input1 ge 1 and \$input2 ge 500 and \$Input3 le 100 and \$Input4 ge 0 and \$Input11 ge 1 and \$Input11 le 2) 3, (default) \$Input1 } </pre>
Output 09: enlarged snow/ice mask			

The operations performed in this step are basically the removal of certain areas from the interim snow mask that were observed to have too low reflectances in the spectral bands used, where also the NDVI plays a role, and the addition of certain pixels to the snow mask (from the original 66 classes derived in Model 1). The latter is partly based on the SWIR band, which - depending on the background reflectance – exhibits relatively low values even in areas with partial snow cover (less than 350 to 400(450)). In areas with high background SWIR reflectance, however, partially snow covered pixels may have SWIR values exceeding even 600 and cannot be retrieved this way without causing too high commission errors. Figure 18 shows an example of the reclassification result over the Alps, with an overall good result, but some of the mentioned confusion between clouds and snow can still be seen on the northern edge of the mountains, where false clouds can be found between the snow.

4.4.3 Separating snow/ice patches from ice clouds

In many instances, snow and ice areas cannot be reliably separated from ice-clouds, which exhibit quite similar spectral properties. Visually, this differentiation is possible in most cases based on structures and colours and also on the geographical location and the general context. However in order to automatically separate these classes, more than pixel-based image reflectance data are necessary.

For this purpose, as a final snow/ice reclassification step, several segment based analyses are performed with the first aim to identify patches that belong to the large scale snow areas, and to separate the snow/ice patches outside the large scale snow/area into those that are most likely snow and ice from those which are more likely ice clouds. The following procedures are applied:

For all snow/cloud patches, it is determined if they contain parts of the large scale snow mask referred to as focsum51x51_snow-ice_thresh_focsum251x51_10km.img (Parameter 21 in Table 2). If they are (partially or fully) within this mask and at the same time fully contained in the second large area snow mask created under 4.4.2, they remain assigned to the snow/ice class. If the objects lie outside the large scale snow/ice mask, they will be assigned to snow/ice or clouds based on the following object-based parameter: Mean SWIR minus 1.5 x SD.

This parameter is based on observations that snow/ice tend to have somewhat lower SWIR values than ice clouds. For each snow/ice patch as a whole in the intermediate result, the SD and the mean are calculated. The SD is multiplied with 1.5 and subtracted from the mean. A threshold of 230 is applied, i.e. snow/ice patches with values below this threshold are identified and taken as snow/ice. In the next step, snow/ice patches plus connected thin and partial snow areas are aggregated, and for each such aggregated patch the percentage of pixels with Mean SWIR minus 1.5 x SD below 230 is determined. If it is above 5%, the entire patch remains snow/ice, if it is below 5%, only the actual snow/ice patch remains snow/ice and the attached thin and partial snow areas are reclassified into clouds or haze.

However, this procedure is of limited success, as it keeps too many ice-clouds classified as snow/ice. It may be more promising to use in addition the parameter band1-3_band1-4_ndi.img (Parameter 11 in Table 2, which accomplishes a rather consistent separation of ice-clouds and surface ice/snow at the large scale, this approach however has not been tested and implemented yet.

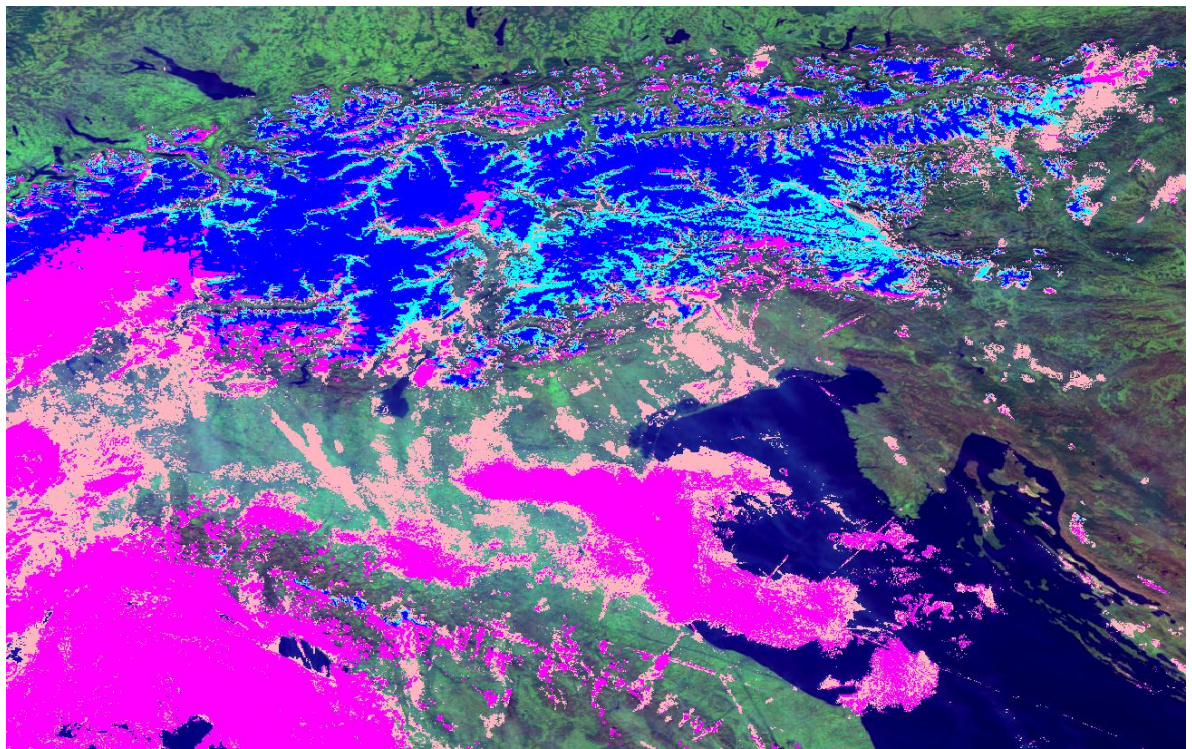
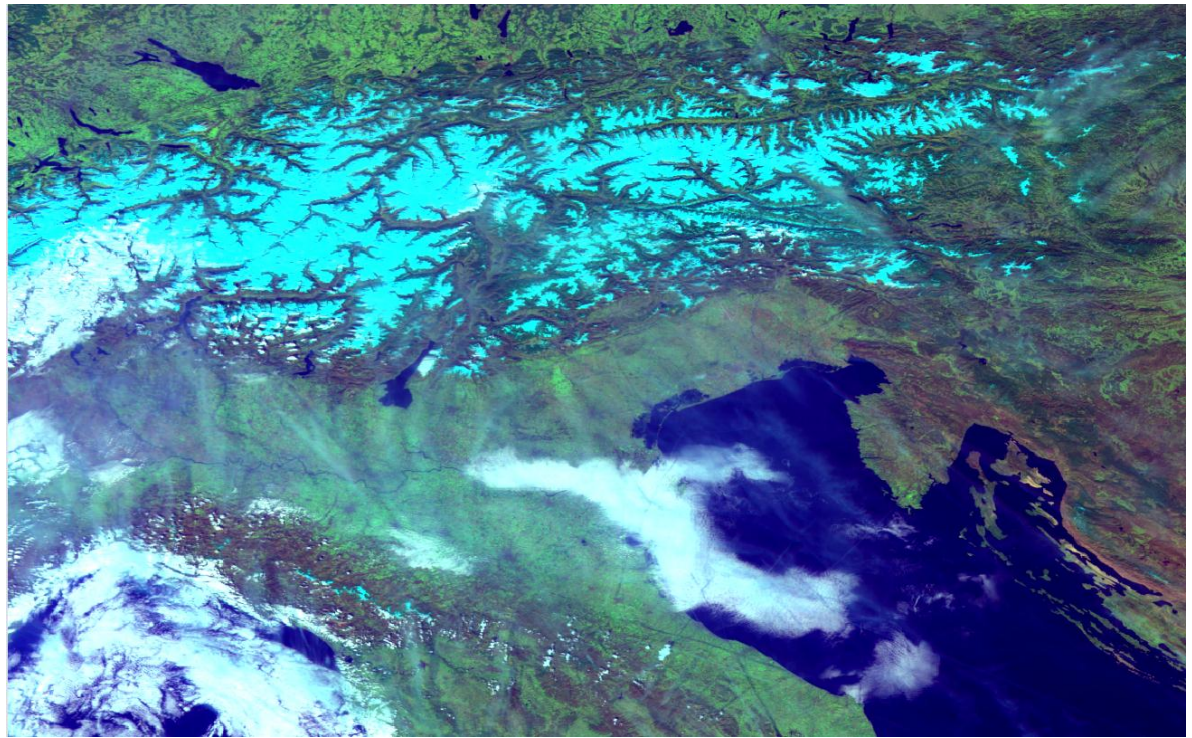


Figure 18: Example of snow/ice (blue) and thin/partial snow/ice (cyan) classes in image probav_l2a_20140321_094455_3_333m_v001.tif of the Alps (March 21, 2014). Magenta: clouds, light pink: haze

4.5 Correcting for the temporal shift of the SWIR band

In chapter 2.1 the temporal shift of the SWIR band recording in relation to the other three Proba-V bands is mentioned, with the consequence that clouds are represented by the area covered by the blue, red and NIR band plus an additional area recorded in the SWIR band only, which extends to the north of the mapped clouds. Neglecting this additional area would lead to an underestimation of clouds in the SWIR band and to the usage of corrupted data in the SWIR band. Therefore, a mechanism has to be found how to include these additional cloud areas.

The cloud detection procedure developed in this work in general leads to a rather complete cloud retrieval including also mixed pixels around the clouds, and thus potentially already including this extended area. Therefore, an automatic addition of a buffer in the north of each cloud may lead to an overrepresentation in some cases. For this reason, the applied procedure aims at an adapted extension of clouds and consists of the following steps:

1. Pixels classified as clear with pixels classified as clouds in their south are identified.
2. The mean of the SWIR band is calculated for each pixel plus the three pixels adjacent to it in the SW, S, and SE, respectively.
3. The quotient of the SWIR value of the pixel considered (center pixel of filter matrix) and the mean SWIR calculated in step 2 is derived.
4. A pixel is assigned to clouds if the conditions listed in Table 12 are met, i.e. if the pixel is clear and has cloud pixels to the south, if the SWIR value of the pixel does not deviate by more than 30% from the calculated average SWIR, if the pixel has a mean euclidean texture value (parameter 7 of Table 2) of at least 30 and if it has a SWIR value of at least 450.

In a second iteration, which turned out to be necessary as the first iteration did not completely fill all these SWIR gaps, step one is repeated, but now pixels are added if they have a SWIR value of at least 450. The correction is applied after the separation of snow and ice from clouds and haze, and only to clouds and haze. Figure 19 shows an example of the SWIR shift and the correction effect.

Table 12: Correction of the SWIR shift

Parameter number (see Table 2)	Raster file name	Input number for operator in Spatial Model	Thresholding Functions defined in Spatial Model Operator (parameters are expressed with their input numbers listed in column 3)
Intermediate output	Clouds and haze (after separating clouds and haze from snow and ice)	1	Conditional { (\$Input1 le 0 and \$Input2 eq 1 and \$Input3 ge 30 and \$Input4 ge 0.7 and \$Input4 le 1.3 and \$Input5 ge 450) \$Input2, (default) \$Input1 }
1	Focal Max filter applied to the cloud mask	2	
7	euctex_b1-3_mean.img	3	
temp	Quotient of the SWIR value of the pixel and the mean SWIR of the pixel and the three neighbouring pixels to the south	4	
4	Proba-v_swir.img	5	
Output: Clouds and haze with SWIR shift correction applied. The result goes into a second iteration adding another cloud pixel if the tested pixel has a SWIR value of at least 450.			

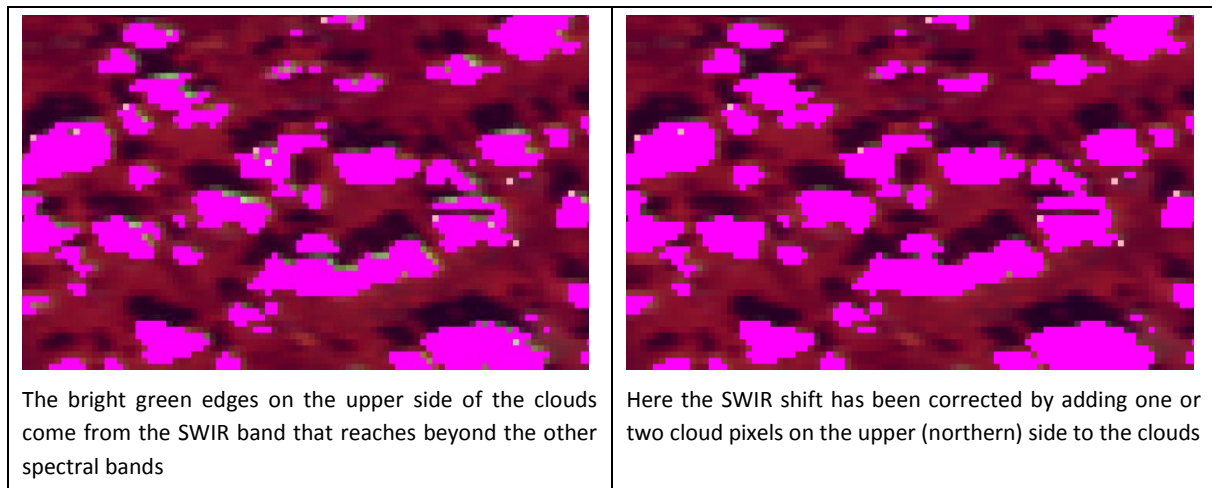


Figure 19: Effect of the correction of the SWIR shift

In a final processing step, the SWIR shift corrected clouds and haze and the snow and ice classes are combined to receive the final result with the classes:

- 0: Nodata and clear areas
- 1: Clouds
- 2: Haze
- 3: Snow and Ice

4: Thin or partial snow and ice cover

5 Summary and Discussion

The proposed cloud and snow/ice mapping approach is an effort to retrieve clouds, haze, and ice and snow as completely and as precisely as possible in a consistent and reproducible way. The methodology consists of thresholding image derived parameters, which consist of multispectral indices (band ratios, band differences, NDIs), texture parameters, and focal parameters derived from intermediate results with moving windows of various sizes. As auxiliary data, the water surfaces of the CCI LC data from 2010 are used.

The developed methodology, as it is based on thresholding image parameters, belongs to the most commonly used cloud screening approaches, examples are provided in [1], [2]. However, the procedure presented in this ATBD is a completely new adaptation of such methods to Proba-V data, and does not incorporate known thresholds or parameter definitions from the literature. It has been developed empirically, step by step, with a trial and error procedure, selecting and interlinking finally the best working and feasible single steps, parameters, thresholds and their combinations. While the algorithm is composed of so many parameters and processing operations, there is still a clear underlying structure, which is shown in Figure 5.

The algorithm is structured into three major processing steps with clearly defined substructures each. The processing has been implemented in the Spatial Model Editor (2016) of ERDAS Imagine, a graphical tool for performing interlinked sequences of image and GIS data processing. The procedure consists of three models that have the following functions:

1. Cloud/haze/snow/ice retrieval producing 66 spectral classes without thematic assignment to either one of the target classes yet
2. Generation of image parameters for the subsequent filtering and thematic assignment
3. Filtering and thematic assignment of the 66 classes derived in (1) to Clouds, Haze, Snow/Ice, and Thin/Partial Snow/Ice, and addition of some cloud pixels in gaps, buffers and water areas

Thus, the output of the algorithm includes the additional class thin/partial snow/ice, which is analogue to haze a class consisting partly to mostly of mixed pixels. The image parameters and thresholds proposed for the definitions of these classes may be a rather optimized version within the development of this specific algorithm, but of course modifications may lead to better results, as by far not all alternatives could be tested or will ever be tested. Nevertheless, even if derived with subjective and arbitrary trial and error methods, the developed algorithm relies on an intense and thorough testing with visual inspections of many results and is based on a longstanding image interpreting experience.

Remaining issues seem especially related to the separation into clouds/haze on the one hand, and snow/ice and respectively thin/partial snow/ice on the other hand. While working out quite well overall, this issue cannot be completely solved with the approaches applied here. Incomplete reclassification of cloud pixels into snow/ice on the one hand, and ice clouds falsely classified as snow/ice on the other hand stay open. But also some other issues remain unsolved, such as commission errors (false clouds) in certain situations, where no practicable way was found to remove them within the applied methodology. Examples include saltlakes and other extreme bright spots (the confusion with bare areas in general cloud be solved), some river valleys (although this could also be largely solved), cities, wetlands, or also agricultural field structures. Change detection using multitemporal data of close acquisition times should be promising for such problems [5], [6]. Omission errors seem to be less of a problem based on visual inspections of the results, though of course there are limitations with regard to the detection of haze, which is also a question of haze definition, which in turn depends on the purposes of the data application.

However, all these are qualitative judgements derived in many instances but not systematically during production. It will be most interesting and relevant, what the systematic visual and quantitative validation efforts will show.

The complexity of the algorithm and the related computation time is a further issue. For operational applications, the algorithm may have to be somewhat simplified or optimized.

6 References

- 1 Lisens, G., P. Kempeneers, F. Fierens, and J. Van Rensbergen (2000). Development of Cloud, Snow, and Shadow Masking Algorithms for VEGETATION Imagery. Proceedings of Geoscience and Remote Sensing Symposium, IGARSS 2000, Honolulu, HI 2: 834–836.
- 2 Wolters, E., Swinnen, E., Benhadj, I., Dierckx, W., PROBA-V cloud detection evaluation and proposed modification, QWG Technical Note, 17/7/2015.
- 3 Wolters, E. , Dierckx, W., Dries, J., Swinnen, E. (2014). PROBA-V Products User Manual v1.1, 7/10/2014.
- 4 Website of the ESA Land Cover Climate Change Initiative <http://www.esa-landcover-cci.org/>
- 5 Eberenz, J., Verbesselt, J., Herold, M., Tsendbazar, NE, Sabatino, G. , Rivolta, G (2016). Evaluating the Potential of PROBA-V Satellite Image Time Series for Improving LC Classification in Semi-Arid African Landscapes. Remote Sens. 8, 987; doi:10.3390/rs8120987.
- 6 Zhu, Z.;Woodcock, C.E. (2014). Automated cloud, cloud shadow, and snow detection in multitemporal Landsat data: An algorithm designed specifically for monitoring land cover change. Remote Sens. Environ., 152, 217–234.
- 7 Pearson, K., Embury, O., Bulgin, C. (2014). Bayesian Cloud Detection Algorithm Theoretical Basis Document. EUM-BC-ATBD-003 Final Issue 1.
- 8 Website of the description of the MODIS Cloud Mask product http://modis-atmos.gsfc.nasa.gov/MOD35_L2/